VHF
COMMUNICATIONS

See the hole where the CF739 fits through the PCB

Second stage 6 x CF739

First stage 6 x CF739

Revisiting the wideband amplifier using the CF739 FET

Guerrino Daipra, ON1EV

Contents

Since the last issue of the magazine I have moved to the seaside in South East England. Publication of the magazine will not be affected.

The response for new articles has been very good so there will be some interesting articles in the magazine this year.

Thank you for your support by subscribing to the magazine for 2011, at the moment the subscription rate is slightly up on last year so that is a good sign.

73s - Andy

Guerrino Daipra, ON1EV

Revisiting the wideband amplifier using the CF739 FET

1.0

Objective

To design a distributed wideband amplifier using the CF739 transistor. The design goal was a low noise amplifier with a minimum gain of 12dB with a bandwidth of 3GHz and an output power of 15dBm.

2.0

Introduction

An amplifier having a wideband and a low noise factor with a respectable output power is common now.

As a good exercise with PUFF and after reading the excellent article in VHF communication magazine "MES-FETish-ism" by Dr Detlef Burchard [1], I thought that I would produce an amplifier using the SMD replacement of the well-known

CF300. I proposed an amplifier using the principle of distributed elements. During the 1950s this kind of amplifier was widely used in the vertical amplifier of the well-known Tektronnix oscillo-scopes. These amplifiers were build around transmission lines realised using lumped elements i.e. inductors with the input and output capacitance of the valve.

3.0

Design

Transmission line theory states that in a transmission line without loss the characteristic impedance is:

$$Zo = \sqrt{L/C} \qquad (1)$$

- Amplifier input impedance is 50Ω

- The active elements have an input capacitance of 1pF

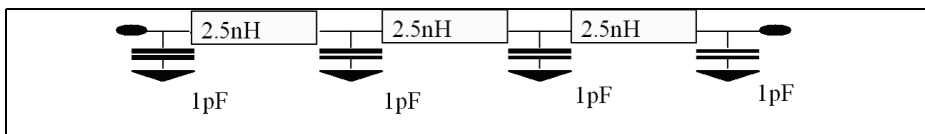We can directly compute the associated inductance:

Fig 1: Transmission line composed of 2.5nH inductors and 1pF capacitors.
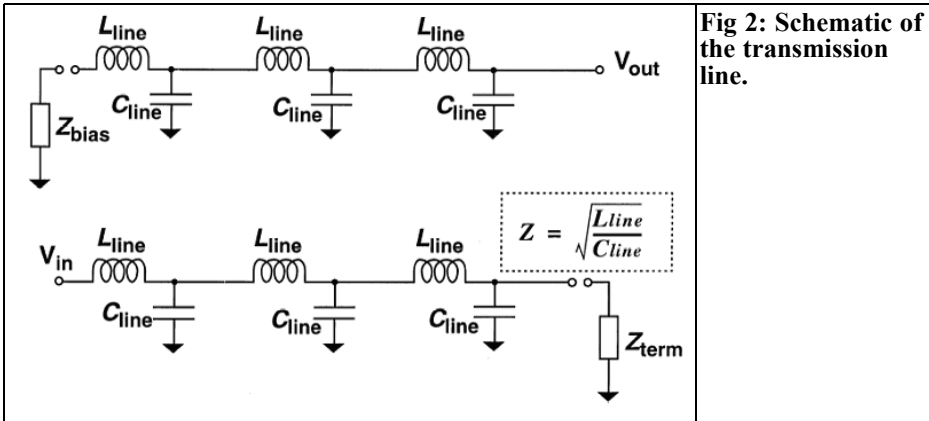
Fig 2: Schematic of the transmission line.

$$L = Zo^2 xC \qquad (2)$$

In our case:

$$2500 * 10^{-12} = 2.5 \times 10^{-9} = 2.5 nH$$

The transmission line will be composed of a series of 2.5nH inductors and capacitors of 1pF (grid–source capacitance of the transistor) as shown in Fig 1.

The next step is to create the microstrip. The following formula gives the length expressed in degrees

$$Length = \frac{Frequency \times induc \tan ce}{Zo} \times 360° \quad (3)$$

In our case the maximum usable frequency of the CF739 is 3GHz.

We choose a characteristic impedance of the microstrip of 100Ω

The electric length is:

$$\frac{3 \times 10^9 \times 2.5 \times 10^{-9}}{100} = 0/075\lambda$$

$$\lambda = 360° \therefore 0.075 \times 360 = 27°$$

The microstrip will be 100Ω and 27° in electrical length. On 1.5mm FR4 substrate the strip width is 0.35mm and length 3.5mm. Fig 2 shows the transmission line.

The theoretical circuit diagram of a distributed amplifier using FET transistors is shown in Fig 3.

How many stages are necessary? Answer: 6 stages will give linear gain of 16 or 12dB.

The gain is given by:

$$G = \frac{g_m^2 Z_{\pi g} Z_{\pi d}}{4} \left(\frac{\sin \frac{N}{2} \left(\beta_g - \beta_d \right)}{\sin \frac{1}{2} \left(\beta_g - \beta_d \right)} \right)^2$$
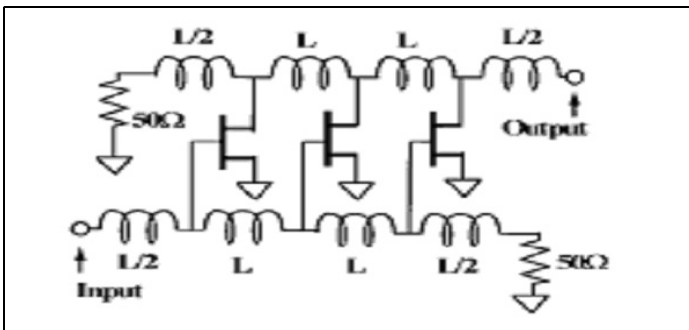

Fig 3: Theoretical circuit diagram of a distributed amplifier using FET transistors.
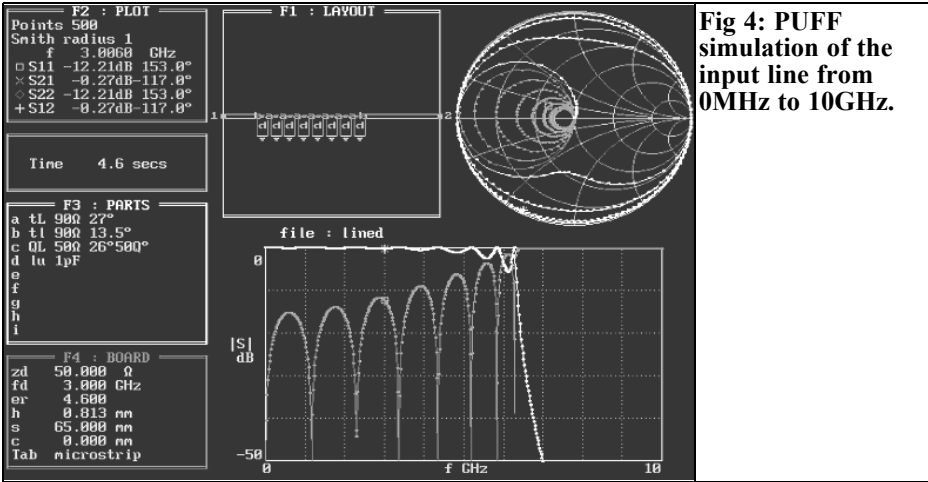
3

Fig 4: PUFF simulation of the input line from 0MHz to 10GHz.

$$G = \left(\frac{N g_m Z_0}{2} \right)^2$$

Where:

- N: number of stages = 6

- Gm: the transconductance of one transistor expressed in A/V, assume a Gm of 25mA/V (25×10^{-3} A/V)

- Zo is the characteristic impedance of the input or output = 50Ω

Linear Gain = $(6 \times 25 \times 10^{-3} \times 50)^2 / 4 = 14$

In dB = 10 log 14 = 11.48dB

Because the same microstrip is used at the input and the output we must add a small capacitor on each transistor drain to

Fig 5: The m derived section described by Pozar [2].

obtain the same propagation constant (velocity).

4.0

Simulation of a transmission line with PUFF program

To verify the theory I have used PUFF to simulate such transmission line. The line structure is build like a PI filter also named "Constant K T section". The simulation of the input line from 0MHz to 10GHz is shown in Fig 4.

The return loss of the line is quite good at the beginning but approaching the maximum frequency; the return loss becomes very bad. What can be done to increase the return loss at those high frequencies?

In Microwave engineering by Pozar page 387 [2] we discover that we can significantly increase the return loss using a little circuit added to the Gate and Drain line section (Fig 5).

L= 2.5nH and C = 1pF
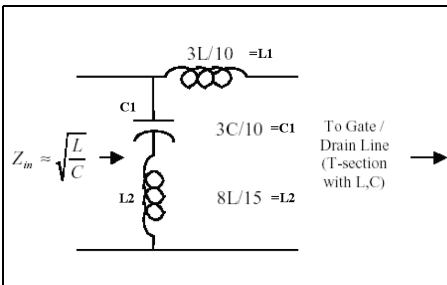
The value of the m derived section is respectively:

4

Fig 6: Simulation of the circuit with an m derived section added.

I use m equal to 0.6 as stated in Pozar's book

L1 = 0.75nH

C1 = 0.3pF

L2 = 1.33nH

A simulation of the new circuit is shown in Fig 6.

Since the theory matches with the simulation we will adopt the new circuit.

The return loss has increased significantly up to 6GHz.

The number of stages is 8 and the return loss is a minimum of 15dB @ 3Ghz and better up to 5GHz.

The next question is why choose the CF739? There are three reasons:

• Still available and low noise.

Fig 7: Simulation of the S parameter file is C9400010.

5
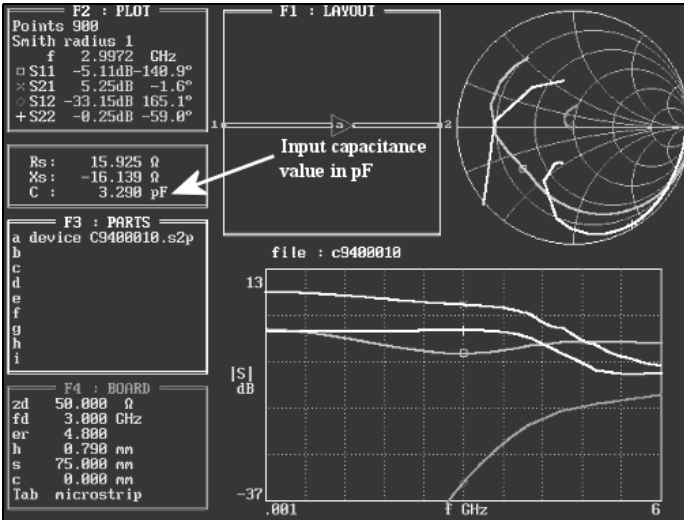
Fig 8: Using PUFF to determine the value of the input capacitance.

- Characterised up to 6GHz

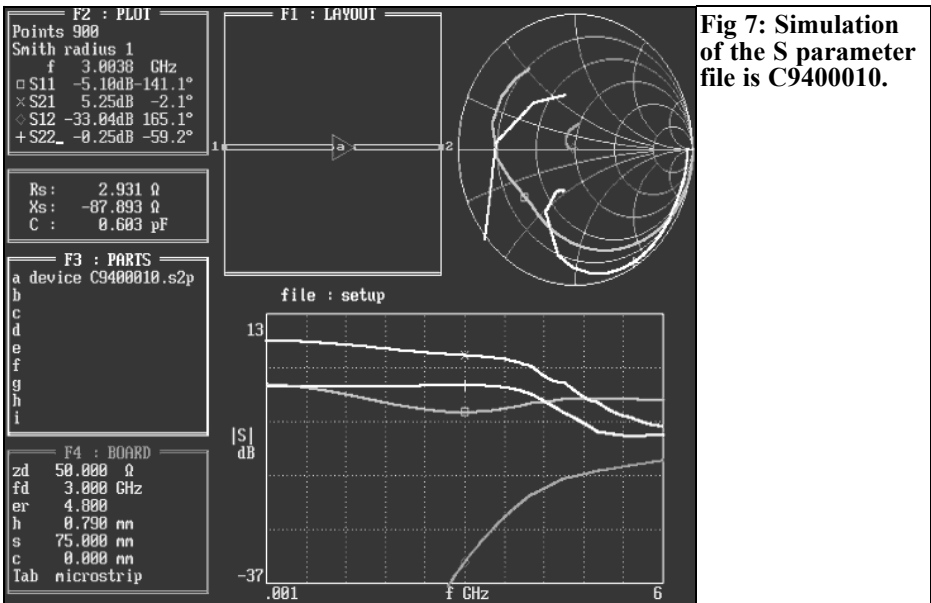- Have a very low S12 parameter that is essential for stability reasons.

I chose the S parameters for the chosen configuration i.e. G2 connected to ground, VDS = 4V, IDS = 10mA, the list found on the Gunthard Kraus web page [3] is very helpful for this. The S param-

eter file is C9400010 (Fig 7).

With the help of PUFF I can retrieve the equivalent parallel capacitor at the chosen frequency. Here is how I retrieve the input capacitance of the transistor (Fig 8):

- In PUFF create a simple file using the chosen transistor.

Fig 9: Using PUFF to determine the value of the output capacitance.

Fig 10: Using PUFF to find the physical dimension of the gate line @ 3GHz.

- Connect the input and the output in PUFF

- Take a SWEEP to produce a graph.
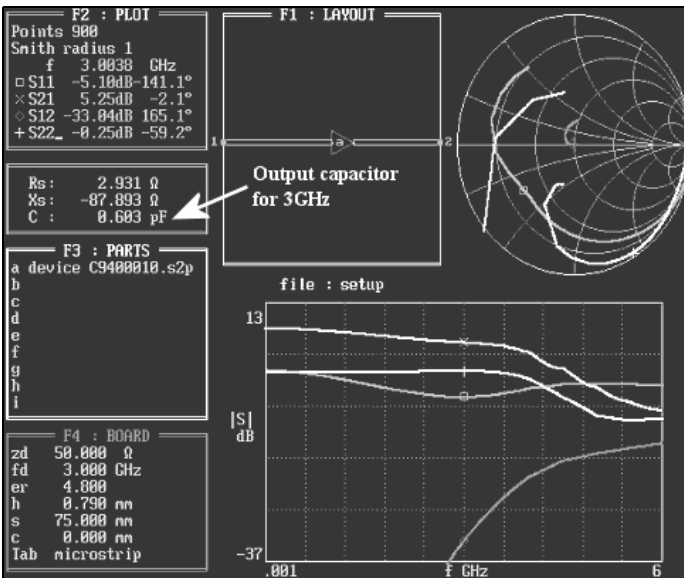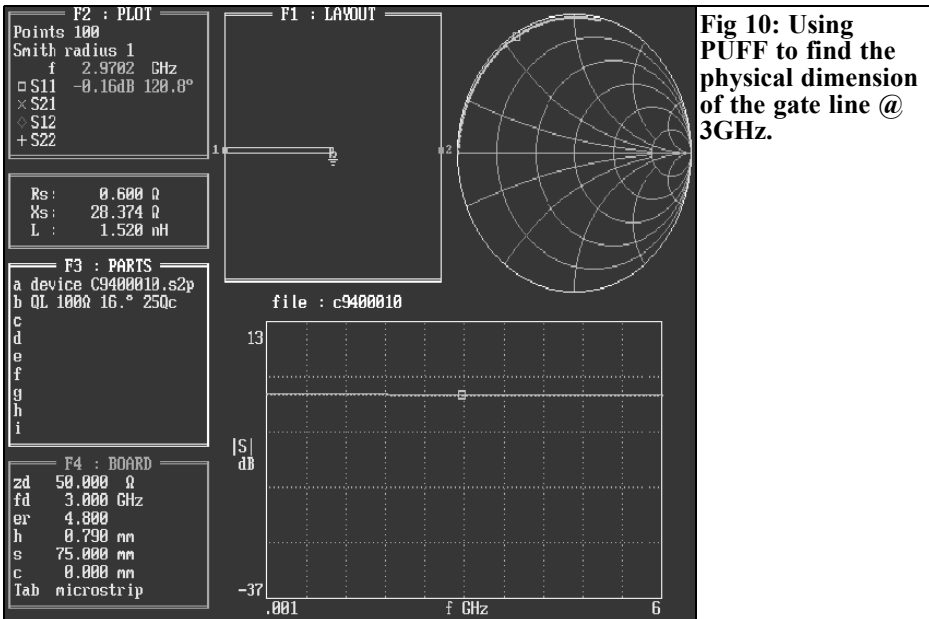
- The Polar and Cartesian values are shown.

- In the window F2 place the cursor after the word S11 and enter =

- In the window under the F2 the equivalent capacitor at the frequency will be shown

The values given at the beginning of the article are wrong. The input capacitance is around 3.3pF @ 3GHz, we are a long way from the value assumed.

The best I could do was to simulate the elements with a real CF739 transistor in lieu of the chosen 1pF capacitor to see if the goal is reachable.

According to equation (1), the value of the electrical length is 118°, this a long way from the rule that states: the electrical length for an inductor must be less than λg/8 (360°/8 = 45°). I could not use

this value. The only way is to create a smaller capacitor using a series capacitor to lower the high capacitance of the input. It can be chosen so that the value equates to the drain output capacitance.

For ease I would like to use the same drain and gate transmission line, therefore I must know the equivalent output capacitance. I used the same method with PUFF (Fig 9) to obtain the value used below i.e. 0.603pF.

Placing a capacitor in series with the gate I obtain this value i.e. 0.603pF. Using the well-known formula gives the following value:

$1/Ceq = 1/C1+1/C2 = 0.603pF$

For C2 = 3.3pF (MAX value)

C1 = 1/0.603-1 /3.3=1.3pF

This is the value to be placed at the input of the gate gives the same value for the Drain or Gate transmission line.

I recalculate the new transmission inductance according to equation (1)
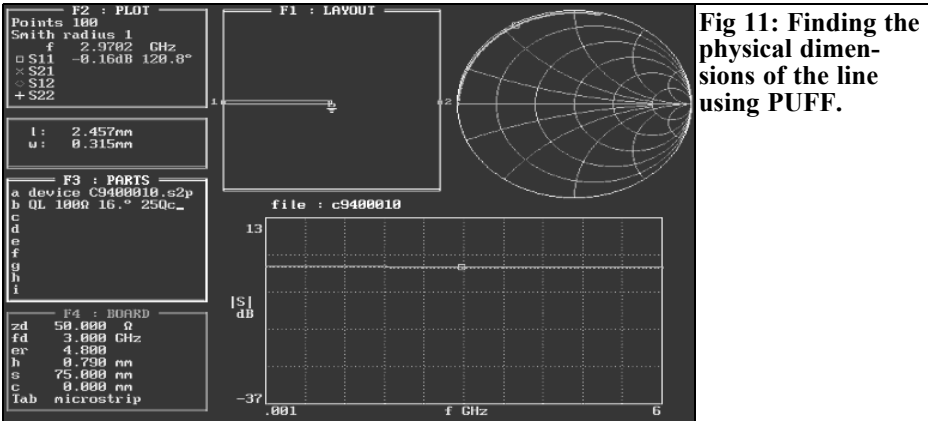
It is:

7

Fig 11: Finding the physical dimensions of the line using PUFF.

2500 x 0.603 x 10^{-12}= 1.5nH

The electrical length is:

1.5 x 10^{-9} x 3 x 10^9/100 = 0.045 of λg

Thus the length in degrees is:

0.045 x 360= 17.7°

The physical dimension for the gate line @ 3GHz is obtained using PUFF (Fig 10). The value is 1.5nH with 16° electrical length.

What are the physicals dimensions? Again with PUFF it is an easy game to play (Fig 11)

The values are directly computed and these values are very small. I think that we have reached the human limit with this value. In the theoretical model of the distributed amplifier it is said that the model is only correct for a unilateral transistor, this transistor must have a very low S12 parameter. That is the case with

this transistor. For a first run, I use PUFF to obtain the frequency response shown in Fig 12.

It is evident that the frequency response is quite flat but sloping. To obtain a flat frequency response I have changed the value of the input capacitor. With a new capacitor of 2.2pF the new response is shown in Fig 13.

5.0

Have we reached the goal?

Not really: the frequency response is more than 3GHz, so we have reached the specification but the gain is not 15dB. For my first attempt I must admit that the m-derived section has not been changed so let's make a try to see if there are any differences?
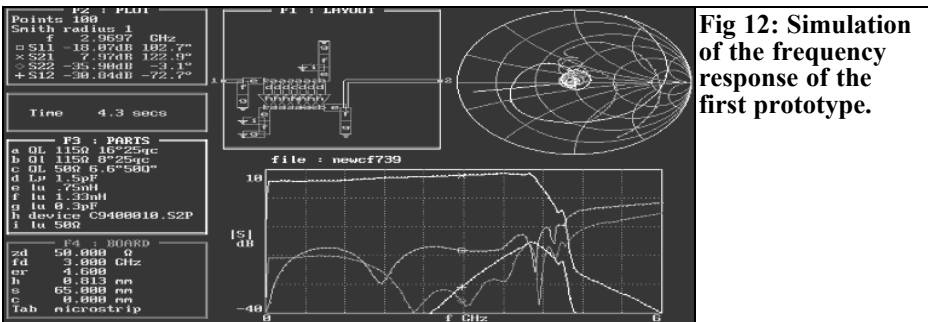

Fig 12: Simulation of the frequency response of the first prototype.
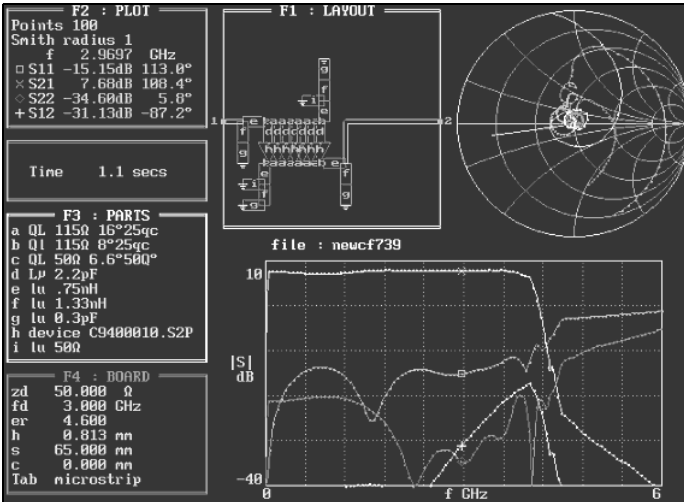
Fig 13: Simulation of the optimised amplifier showing a flatter frequency response.
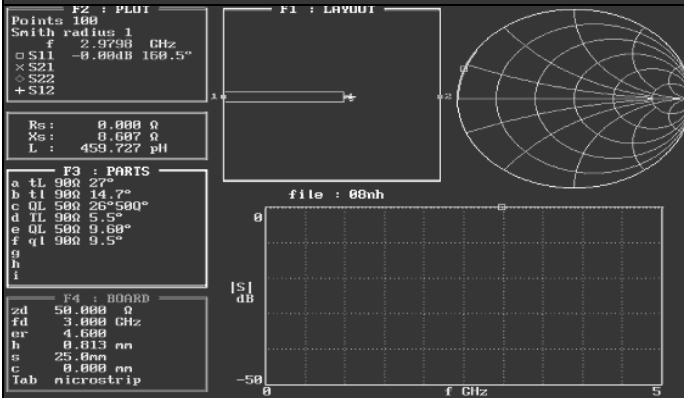
Fig 14: Dimensions of L1 (see text).
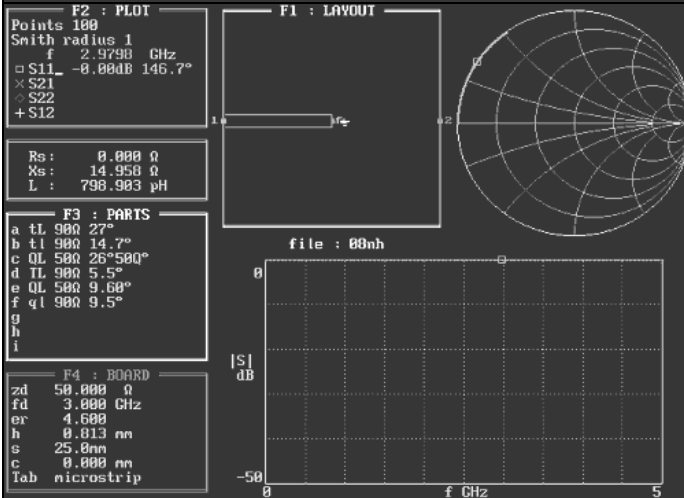
Fig 15: Dimensions of L2 (see text).
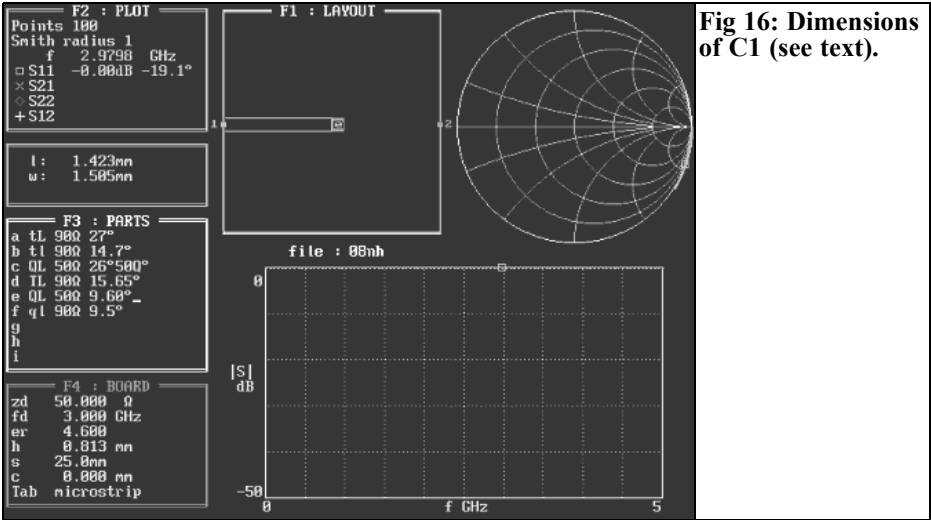
Fig 16: Dimensions of C1 (see text).

The values for this section according to Pozar are:

- **L1 = 0.45nH**

- Z = 90Ω + 5.5°

The dimensions are: (see Fig 14)

- L = 0.8mm

- W = 0.45mm

- **L2 = 0.8nH**

- Z = 90Ω + 9.5°

The dimensions are: (see Fig 15)

- L= 1.47mm

- W= 0.45mm

- **C1 = 0.18pF**

- Z = 50Ω + 9.6°

The dimensions are: (see Fig 16)

- L = 1.42mm

- W= 1.5mm
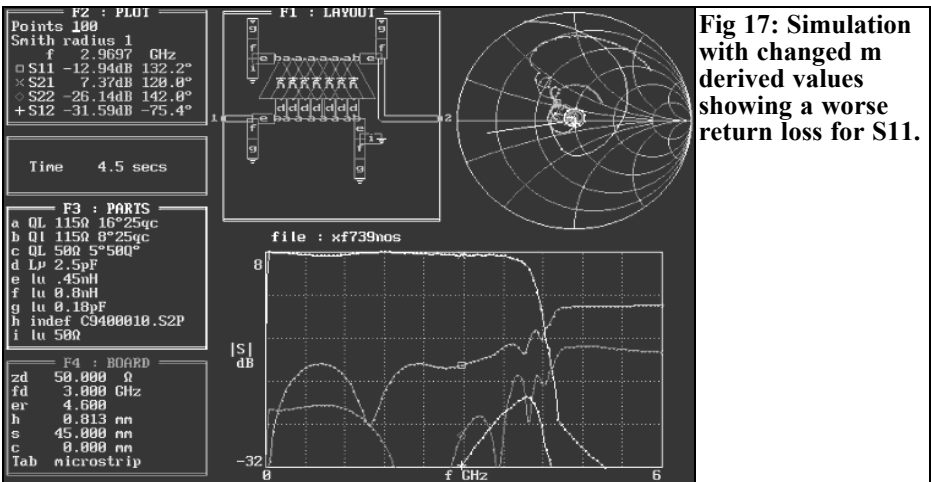
Fig 17: Simulation with changed m derived values showing a worse return loss for S11.
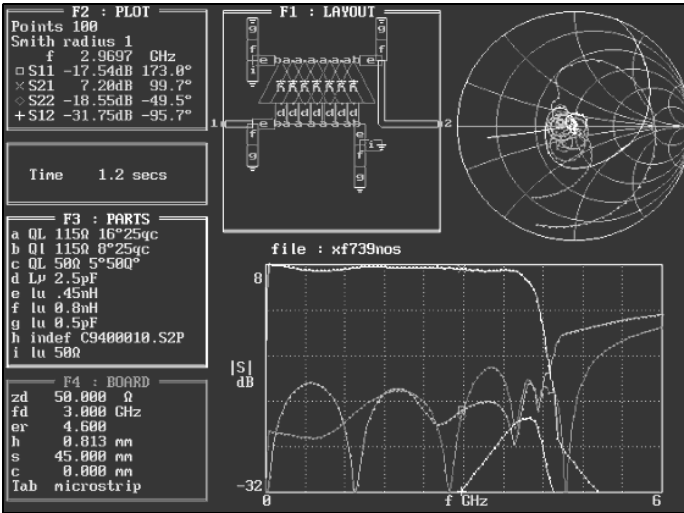
Fig 18: Simulation of optimised circuit showing an increased return loss of -17dB for S11.

```
F2 : PLOT
Points 100
Smith radius 1
    f    2.9697  GHz
□ S11 -17.54dB 173.0°
× S21   7.20dB  99.7°
◇ S22 -18.55dB -49.5°
+ S12 -31.75dB -95.7°

Time    1.2 secs

F3 : PARTS
a QL 115Ω 16°25qc
b Q1 115Ω 8°25qc
c QL 50Ω 5°50Q°
d Lµ 2.5pF
e lu .45nH
f lu 0.8nH
g lu 0.5pF
h indef C9400010.S2P
i lu 50Ω

F4 : BOARD
zd  50.000  Ω
fd   3.000 GHz
er   4.600
h    0.813 mm
s   45.000 mm
c    0.000 mm
Tab  microstrip

F1 : LAYOUT

file : xf739nos
```

Using the new values for the m-derived section I made a new sweep with the new values as shown in Fig 17. The values have changed and the return loss is worse than before for S11. Optimising the values gives a return loss that has increased

Fig 19: Picture of 10-stage prototype amplifier.
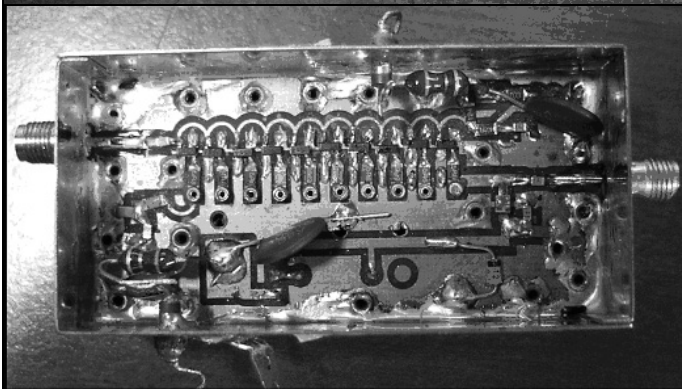
Fig 20: Picture of 10-stage prototype amplifier.
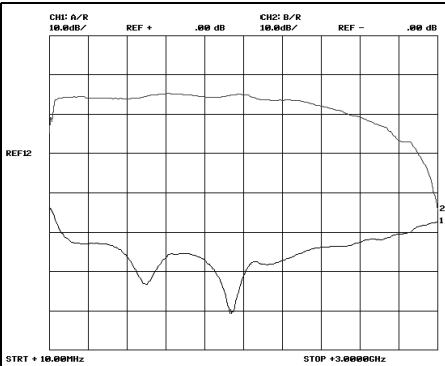
Fig 21: Measured results on 10-stage amplifier.
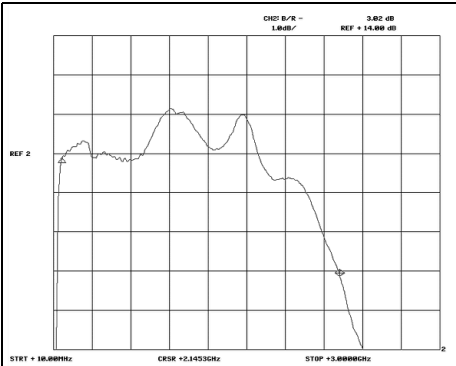
Fig 22: Gain of 10-stage amplifier measured with an HP8756A and HP8350B/HP8325A, 1dB/div.
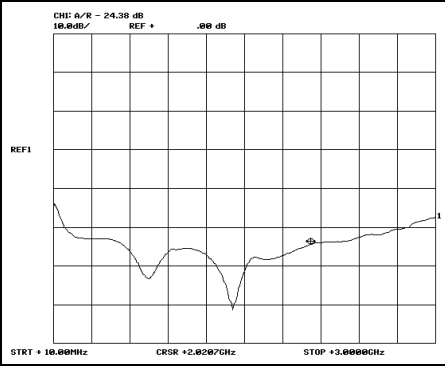
Fig 23: Return loss measured with an HP8756A and HP8350B/HP8325A,

to -17dB for S11 (Fig 18)

The last generation is now quite good but how can the small transmission line dimension be handled? The price to pay with a greater bandwidth is a smaller gain.

6.0

Conclusion
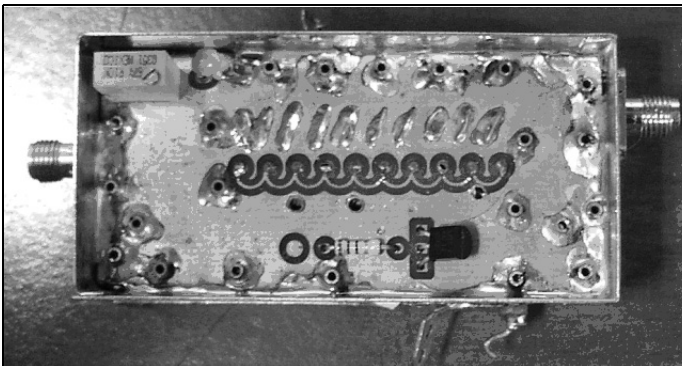
First of all I must admit that the goal has not been reached, there are a few other assumptions that must be taken into account.

The source leg of the transistor was connected directly to ground in my first try.

Normally I would evaluate the actual value of the "via" used to ground the transistor.

The gain obtained in this configuration is lower than the other c9501525.s2p file available from the Gunthard Kraus's website [3].
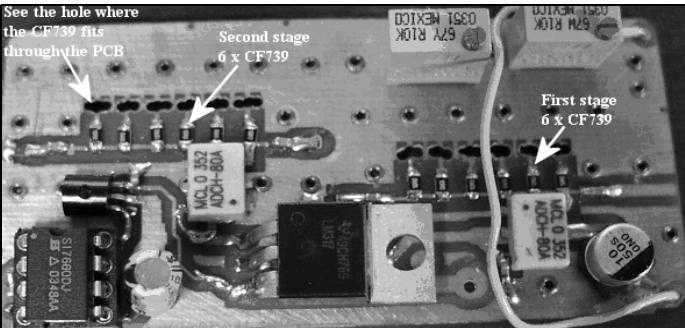
Fig 24: Picture of a prototype using two 6-stage amplifiers with a gain expected of around 20dB.
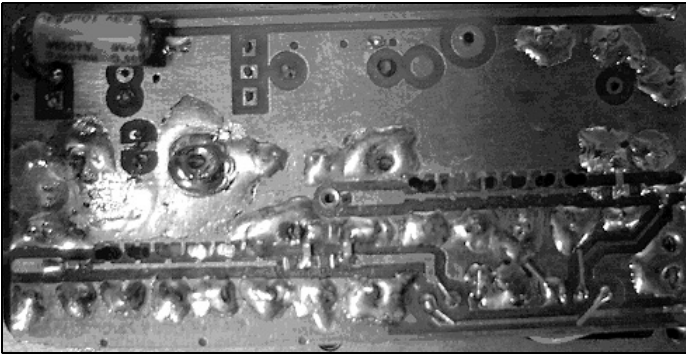
Fig 25: Picture of a prototype using two 6-stage amplifiers with a gain expected of around 20dB.

A better transistor gives a better frequency response but gives more chance to instability

The dimensions the microstrip line implies another way of placing the CF739 transistor. It was placed vertically through the printed circuit board, this way the transistor legs take up minimum surface area.

The second prototype shows the influence of grounding the source, it is actually the most important aspect of this amplifier regarding stability.

Fig 19 and 20 show the first prototype of a 10-stage amplifier and Figs 21 – 23 show the measured results.

Figs 24 and 25 show a prototype using two 6-stage amplifiers with a gain expected of around 20dB. Fig 26 shows the circuit diagram of the 6-stage amplifier.
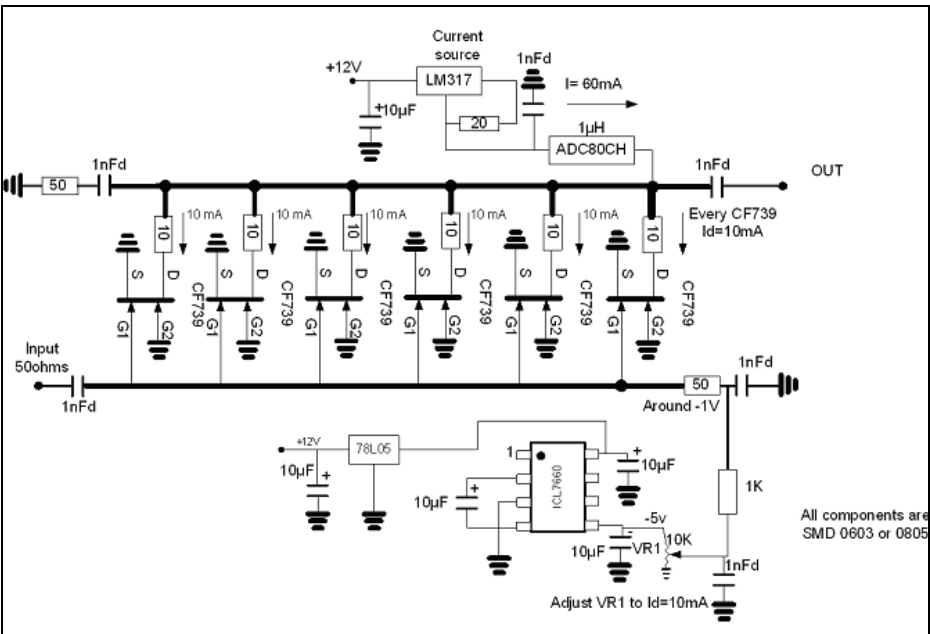

Fig 26: Circuit diagram of the 6-stage amplifier.

7.0

Appendix CF739 Data

Figs 27 – 29 show the CF739 Data

SIEMENS   CF 739

Electrical Characteristics
at T_A = 25 °C, unless otherwise specified.

Parameter	Symbol	min.	typ.	max.	Unit
DC Characteristics					
Drain-source breakdown voltage I_D = 100 µA, $- V_{G1S}$ = $- V_{G2S}$ = 4 V	$V_{(BR)DS}$	10	–	–	V
Gate 1 leakage current $- V_{G1S}$ = 5 V, V_{G2S} = V_{DS} = 0	$- I_{G1SS}$	–	–	20	µA
Gate 2 leakage current $- V_{G2S}$ = 5 V, V_{G1S} = V_{DS} = 0	$- I_{G2SS}$	–	–	20	
Drain current V_{G1S} = 0, V_{G2S} = 0, V_{DS} = 3 V	I_{DSS}	6	–	60	mA
Gate 1-source pinch-off voltage V_{G2S} = 0, V_{DS} = 5 V, I_D = 200 µA	$- V_{G1S(P)}$	–	–	2.5	V
Gate 2-source pinch-off voltage V_{G1S} = 0, V_{DS} = 5 V, I_D = 200 µA	$- V_{G2S(P)}$	–	–	2.5	
AC Characteristics					
Forward transconductance V_{DS} = 5 V, V_{G2S} = 2 V, I_D = 10 mA, f = 1 kHz	g_{fs}	–	25	–	mS
Gate 1 input capacitance V_{G2S} = 2 V, V_{DS} = 5 V, I_D = 10 mA, f = 1 MHz	C_{g1ss}	–	0.95	–	pF
Output capacitance V_{G2S} = 2 V, V_{DS} = 5 V, I_D = 10 mA, f = 1 MHz	C_{dss}	–	0.5	–	
Noise figure V_{G2S} = 2 V, V_{DS} = 5 V, I_D = 10 mA, f = 1.75 GHz V_{G2S} = 2 V, V_{DS} = 5 V, I_D = 10 mA, f = 800 MHz	F	– –	1.8 1.1	– –	dB
Power gain V_{G2S} = 2 V, V_{DS} = 5 V, I_D = 10 mA, f = 1.75 GHz V_{G2S} = 2 V, V_{DS} = 5 V, I_D = 10 mA, f = 800 MHz	G_{ps}	– –	17 22	– –	
Control range V_{G2S} = 2 V … – 3 V	ΔG_{ps}	–	50	–	

Fig 27: Electrical characteristics of the CF739.

SIEMENS CF 739

Common Source S-Parameters, G₂ RF grounded

f GHz	S_{11} MAG	ANG	S_{21} MAG	ANG	S_{12} MAG	ANG	S_{22} MAG	ANG
			V_{DS} = 5 V, V_{GS} = 2 V, I_D = 10 mA, Z_0 = 50 Ω					
0.06	0.999	− 2.4	3.21	176.9	0.001	81.8	0.963	− 1.0
0.08	0.998	− 3.2	3.21	175.5	0.001	85.8	0.963	− 1.4
0.10	0.998	− 4.1	3.21	174.3	0.001	90.8	0.962	− 1.7
0.15	0.997	− 6.0	3.22	171.4	0.002	84.2	0.962	− 2.5
0.20	0.993	− 8.0	3.22	168.4	0.002	88.1	0.962	− 3.4
0.25	0.989	− 10.1	3.21	165.5	0.003	84.4	0.962	− 4.3
0.30	0.987	− 12.1	3.21	162.5	0.003	83.3	0.962	− 5.2
0.40	0.975	− 16.0	3.18	156.6	0.004	79.6	0.961	− 6.8
0.50	0.965	− 19.9	3.15	150.7	0.005	78.6	0.960	− 8.5
0.60	0.951	− 23.8	3.12	145.0	0.006	78.0	0.960	− 10.3
0.70	0.935	− 27.5	3.09	139.3	0.007	76.6	0.961	− 12.0
0.80	0.918	− 31.4	3.05	134.0	0.008	73.3	0.958	− 13.7
0.90	0.900	− 35.2	3.03	128.5	0.009	70.4	0.956	− 15.4
1.00	0.877	− 39.0	3.02	122.9	0.009	69.5	0.955	− 17.0
1.20	0.883	− 46.6	2.96	111.4	0.010	66.4	0.953	− 20.6
1.40	0.773	− 53.7	2.85	99.7	0.011	59.9	0.949	− 24.3
1.50	0.744	− 56.8	2.77	94.4	0.012	59.9	0.949	− 26.2
1.60	0.720	− 60.1	2.74	89.2	0.012	57.5	0.949	− 27.9
1.80	0.666	− 66.2	2.64	78.9	0.012	54.1	0.948	− 31.5
2.00	0.614	− 72.8	2.59	68.6	0.012	49.2	0.945	− 35.3
2.20	0.556	− 80.3	2.53	57.4	0.012	43.7	0.941	− 39.4
2.40	0.497	− 87.2	2.45	45.6	0.010	39.4	0.937	− 44.4
2.50	0.466	− 90.2	2.38	40.0	0.009	35.2	0.936	− 47.0
2.60	0.449	− 92.8	2.34	34.5	0.008	32.2	0.936	− 49.6
2.80	0.408	− 97.1	2.24	23.6	0.005	25.1	0.937	− 54.6
3.00	0.375	− 101.7	2.17	12.2	0.002	− 25.0	0.934	− 59.1

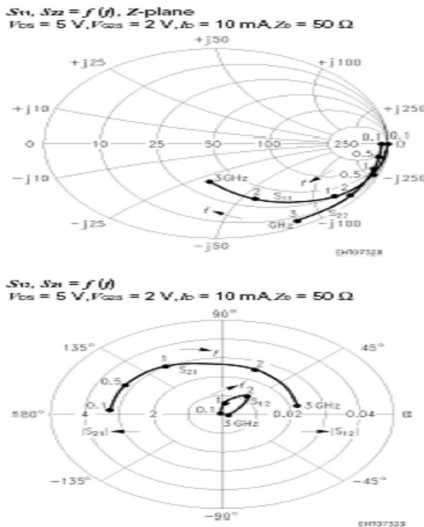**Fig 28:**
S parameters for the CF739.

Fig 29: Smith charts for the CF739.

8.0

References

[1] MES-FETishism, Detlef Burchard, VHF Communications Magazine, Part I 1992/3 pp 183 − 188, Part II 1992/4 pp 232 − 240, Part III 1993/2 pp 66 - 72

[2] Microwave engineering Third Edition Wiley and Sons ISBN 9812-53-186-6

[3] Guthard Kraus web page: http://www.elektronikschule.de/~krausg/

André Jamet, F9HX

Dielectric absorption or how not be electrocuted !

1.0

Introduction

This article presents a phenomena that is not well know and not good for very sensitive electronic devices. However, it underlines an unrecognised danger when using high DC voltages. Because our valve PA can work at kilovolts the danger is quite obvious despite usual precautionary measures taken during setting up, repairs or maintenance, as we will see later.

2.0

"The capacitor"

All of us know what a capacitor does. After all, it is only two electrodes separated by an insulating material. Fig 1 shows the equivalent model including parasitic elements. We can see the series resistance that represents the resistive losses in the connections and in the dielectric. The connections and the length of the electrodes form the parasitic inductance, this is important for high frequencies. Parallel resistance comes mainly from the capacitor body surface therefore dependant on the ambient hu-

midity and pollution. For aluminium and tantalum capacitors the electrolytic solution causes a leakage depending on voltage and temperature. That kind of parallel resistance is a real nuisance in interstages amplifiers.

3.0

The Dielectric Absorption (DA)

The dielectric absorption or soakage is a phenomenon that we can notice with capacitors. It is not new.

The manifestation of DA was found as early as the 1700s by old experimenters using a capacitor such a Leyden jar (Fig 2) and an electrostatic machine like a Wimshurst machine (Fig 3). It is a glass jar with metal foil electrodes inside and out. When they charged the capacitor up to a high voltage, they knew if they
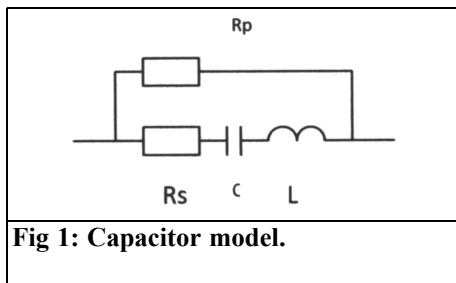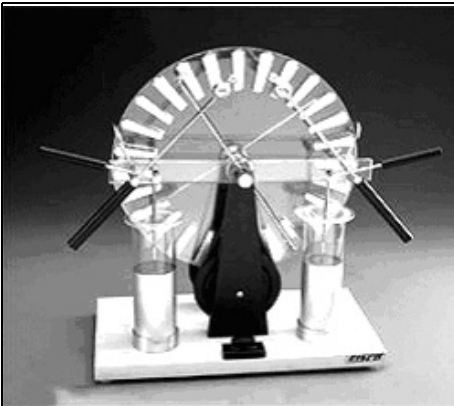

Fig 1: Capacitor model.

Fig 2: Wimshurst electrostatic machine.

Fig 3: Leyden jar.

shorted out the capacitor, the charge would go away. But if they shorted out the capacitor for only a short time, the voltage would recover and they learnt that to their cost!

4.0

A touch of theory

The theory of dielectrics provides a fairly good explanation of how the molecules are slowly polarised to store charge and how they slow to let loose of their polarisation when the original voltage is removed [1]. All capacitors have some DA, but there are enormous difference depending of the dielectric and the manu-
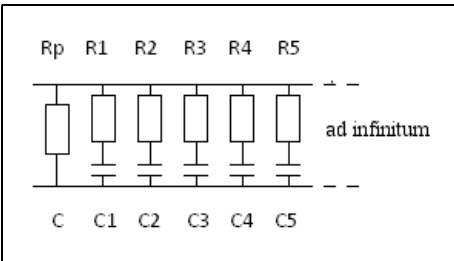

Fig 4: DA model.

facturing process.

Paul C. Dow Jr [2] has established a model to represent a capacitor having some DA. Fig 4 shows that model without the parasitic inductance because it does not play any role in the DA explanation. We can see several RC circuits in parallel with an ideal capacity C with its leakage resistor R.

To establish the various RC circuits, measurements are done with switches using the following sequence:

1 Apply voltage to the capacitor C

2 Open circuit the capacitor C

3 Short circuit the capacitor C

4 Monitor the capacitor C voltage

5 Eventually short circuit again

6 Monitor the capacitor C voltage

Results depend on the duration of each step. Usually, step 1 is long enough to reach a capacitor full charge. Steps 3 and 5 have to be short but without too large a discharge current, not enough to damage the capacitor.

Plotting the residual voltage from a few milliseconds up to several minutes, the curve is not a simple exponential. We can calculate, from the successive steps,

Table 1: F9HX measurements.

Type	Charging Voltage	1st short-circuit					2nd short-circuit			
		Residual voltage %					Residual voltage %			
	volts	10s	1m	5m	10m	15m	10s	1m	10m	15m
Dipped tantalum 100µF 20V	16	1	3.6	5.6	6	6.1	0.25	0.8		
Aluminium 22µF 350V	162	0.8	2.0	2.8	2.8	2.7	0.09	0.15		
Aluminium 10µF 16V	12	1.5	2.3	4.1	4.7	5.5	0.08	0.23	0.63	1.12
Metalised paper 10µF 63V	100	0.12	0.6	1.24	1.35	1.33	0.01	0.05	0.13	0.21
Metalised polyester 10µF 63V	16	0.06	0.11	0.13						

several time constants. They are quite unexpected. For example, with a 1µF metallised polyester capacitor, we can obtain:

$R = 5 \times 10^{12}\Omega$ $R1 = 3.5 \times 10^{12}\Omega$
$R2 = 2.5 \times 10^{11}\Omega$ $R3 = 2 \times 10^{10}\Omega$
$R4 = 3 \times 10^{9}\Omega$ $R5 = 3.3 \times 10^{8}\Omega$
$C = 1µF$ $C1 = 140pF$
$C2 = 200pF$ $C3 = 270pF$
$C4 = 193pF$ $C5 = 120pF$

$RC = 5 \times 10^{6}s$ self-discharge time constant
$R1C1 = 490s$ first DA time constant
$R2C2 = 50s$ second DA time constant
$R3C3 = 5.4s$ third DA time constant
$R4C4 = 0.6s$ fourth DA time constant
$R5C5 = 0.04s$ fifth DA time constant

Usually, DA is expressed in percentage:

(%) DA =   (residual voltage / charging voltage) x 100.

DA increases when the charge time is increased and the discharge time reduced. The DA can be from 1% up to 20% according to the dielectric.

The other references give typical values for various kinds of dielectrics. It is obvious that Teflon, polystyrene, polyethylene, Mylar, and low-k ceramics, have low DA. On the contrary, oil or PCB impregnated paper, high-k ceramics and electrolytic show high DA.

5.0
My measurements

It was not my intention to reproduce that eminent scientists well designed measurements. So, I did some experimentation to observe the phenomenon. Without an automatic device giving the steps and setting on/off neither switches, nor a recorder for the capacitor voltage, I did my measurements "by hand". So, as it is

very tedious, I only made a few tests.

Successively, I charged some capacitors, then open the circuit, then short-circuit the capacitor, and measured the residual voltage. A 100MΩ digital voltmeter was used to measure the capacitor voltage. There is a limit to the residual voltage measurement because the DA has to supply the voltmeter. With this kind of voltmeter, the discharge time constant is:

$T = 10^8 \times 10^{-5} = 100$ seconds
= 1.66 minutes for a 1µF capacitor.

Therefore, we cannot know the actual voltage for times exceeding one minute. On the contrary, for larger capacities, we are able to follow the voltage change for longer durations.

As anticipated, the phenomenon is easy to observe. Low loss dielectric capacitors have shown the lowest DA see the Table 1.

6.0

DA and analogical circuits

DA characteristics are obviously detrimental in applications involving sample/hold and numerous papers are available.

Low DA CMS capacitors can be questionable since NPO/COGs are only available for quite small values. Therefore, space can be provided to insert low DA leaded capacitors.

Cancellation circuits can improve sample/hold circuits [3,4] but they do not concern the usual amateur radio field.

7.0

DA and Hi-Fi

"golden-ears" say that they can hear the benefit of low DA capacitors as inter-stage coupling in amplifiers. Obviously electrolytic capacitors should not be used for that application. On the contrary, for loudspeaker cables it is more questionable.

There were endless discussions between "golden-ears" and engineers on the strange effects of DA on Hi-Fi. For myself, I do not want to take a stand in this "war" but I am prepared to accept any strange effect. Experience of amateur radio has shown that the impossible is not always true!

8.0

DA and RF

We are lucky because low DA dielectrics are also low loss for RF. For example, Teflon is able to make good PCB up to hyper frequencies. I didn't find a lot of articles on that subject but did find that VCOs can suffer from high DA dielectrics.

9.0

How not to be electrocuted

For safety, our high voltage power supplies have a bleeder to discharge the capacitors when the mains electricity is off. Normally, there is no risk for the operator during repair or maintenance because the capacitors are discharged. In practice, a bleeder is a wire wound resistor and if Murphy is alive, wire can be cut! Nobody knows if this has hap-

pened and it is a great danger for the operator because the capacitors are not discharged!

If the operator is skilled and prudent, he makes a temporary short-circuit with an isolated screwdriver between the DC outputs of this power supply. Unfortunately, if the capacitor DA is high enough the residual voltage could be dangerous. For example 10% of 2000 volts is 200 volts which is dangerous in some circumstances.

What can we do? First of all put two resistors in parallel as bleeders, half power rating and twice the ohmic value. If one is open, the other remains.

Moreover, advice from a man having a great experience in high voltage power supplies. The best way to avoid any risk is to make a permanent short-circuit during any work on those devices. Eventually you will short-circuit the full voltage and what a mess! Anyway that's better than to be electrocuted!

One more piece of advice: if you turn off a cathode-ray tube TV set and open up the back, what is the first thing you have to do before you start working on it? Put a permanent grounding strap on the HV plug.

10.0

Conclusion

DA is not a well-known phenomenon. In some cases it can play an important role in capacitors utilisation.

11.0

References

[1] The Art of Electronics, Paul Horowitz & Winfield Hill, Cambridge University Press

[2] An analysis of certain errors in electronic differential analyzers, IRE Transactions on Electrical Computers, March 1958

[3] What's All This Soakage Stuff, Anyhow? Bob Pease, Electronic Design, May 13, 1998

[4] Modeling Dielectric Absorption in Capacitors, Ken Kundert, the Designer Guide Community, 2/01/2008

[5] Understand Capacitor Soakage to Optimise Analog Systems, Bob Pease, 1982, http://www.national.com/ rap/application/0,1570,28,00.html

[6] Circuit Design Consideration for Low Dielectric Adsorption Applications, Wayne Canning, and www.ascapacitor.com

[7] Dispersion and Absorption in Dielectrics, KS Cole & RH Cole, Journal of chemical Physics, 2/1942

Gunthard Kraus, DG8GB

An interesting program: Simulation of RF circuits with LTspice IV, part 3 of 3

Continuation from issue 4/2010

7.0

Investigation of the complete circuit

7.1. Preparation

It begins with some work because the complete circuit, consisting of the preamplifier, mixer and bandpass filter, must be entered using the LTspice editor (Fig 40). The best place to start is with the preamplifier; hopefully this still exists as an LTspice project on your PC. If it does, store it under a new name and add the other two stages. The output is labelled "IF_OUT" and a sine wave signal with 20mV peak value with a centre frequency of 137MHz is connected to the RF input. The LO signal is a sine wave but 37MHz at 2V peak value. The supply voltage of the preamplifier is +9V.

The simulation will be for 20µs with a "Maximum Time Step" of 0.1ns that gives 20µs/0.1ns = 200,000 samples available for the FFT. Do not forget to switch off the data compression. Also always ensure that the following check takes place:

- Press the hammer shaped button on the control panel to get the SPICE record form. On the left the check box marked "Gear" under "Default Integration Method" MUST be

checked and active. Otherwise there will be simulation problems at high frequencies and with complex circuits, including infinitely long simulation times or even causing the program to abort. Please make this check regularly particularly when starting a new project or if the schematic has been modified. Sometimes in such a case the program changes without announcement.....

7.2. Determining the overall gain at the centre frequency

Fig 40 gives the peak value of the IF_OUT signal (37.5mV). This equates to an incident wave of 10mV (half source voltage value) applied.

That results in an S21 for the converter of 37.5 mV/10mV = 3.75 or 11.5dB.

A rough calculation to verify S21 using the values of the individual stages:

$$\begin{aligned} \text{S21 in dB} \quad &= \quad \text{preamplifier gain -} \\ & \qquad \text{mixer attenuation -} \\ & \qquad \text{filter attenuation} \\ &= \quad 25 - 4.5 - 8 \\ &= \quad 12.5\text{dB.} \end{aligned}$$

The deviation of 1dB comes from mismatches between the individual stages and in practice there will be at least 1 to 2dB loss of gain because in the simulation the mixer transformers are taken as ideal.
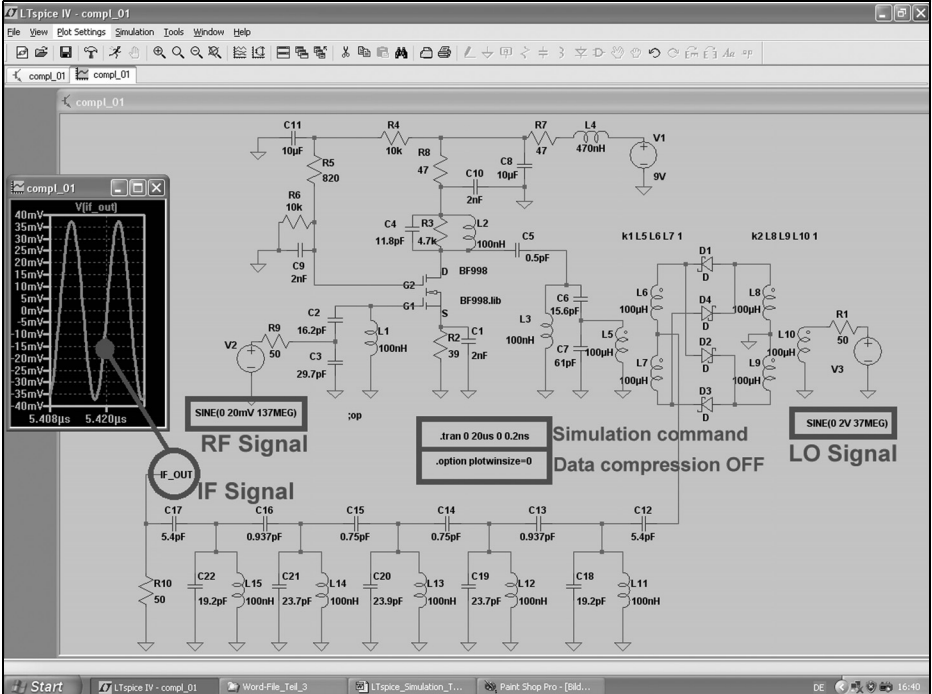
Fig 40: Drawing this circuit takes a fair amount of work but it is the key to the interesting simulation of the circuit characteristics.

7.3. Determining the transmission curve of the converter

7.3.1. Simulation using individual spectral lines

This is not so simple because the AC-Sweep fails when it finds a frequency conversion by the Double Balance Mixer (DBM) because everything takes place in the time interval.

Thus we must use a trick and feed the RF input with a range of equal large signals i.e. 136/136.5/137/137.5/138MHz that cover the pass band. A diagram with the
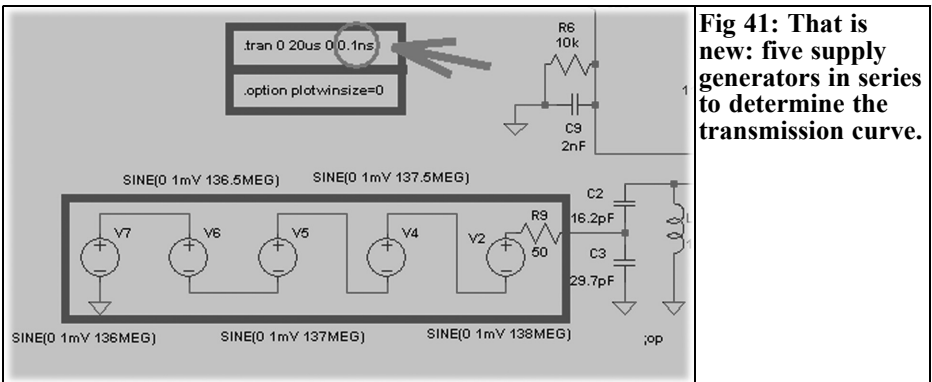
Fig 41: That is new: five supply generators in series to determine the transmission curve.
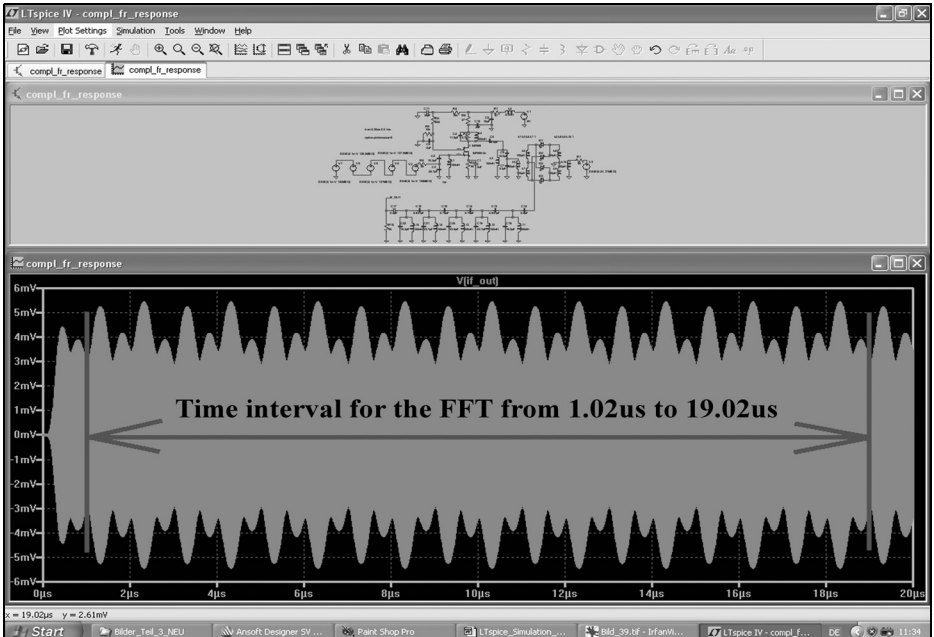
Fig 42: After the simulation the time slot for the FFT of the output signal is selected.

change required can be seen in Fig 41. A quite small peak value of 1mV was selected for each single signal in order to avoid over driving or intermodulation effects. With a "Time Step" of 0.1ns and a simulation time of 20µs, 200,000 genuine samples are available and 131,072 can be used for the FFT. The usual settings are used: the data compression is switched off and "Gear" Integration must not be forgotten. That gives a screen as shown in Fig 42.

The first 1µs at the beginning must be ignored for the FFT (because this is the "settling time" of the circuit before idling) and so the FFT time slot is selected to a value of 18µs (from 1.02µs to 19.02µs - between the two zero crossings of the voltage). Fig 43 supplies sufficient information about the total transmission curve with a maximum level difference of approximately 1.5dB. The practical man would immediately adjust the circuit to correct the somewhat

too high centre frequency of the transmission curve!

7.3.2. Frequency response measurement using a Dirac pulse

This modern technology only became possible with the rapid advancements of communication and computer technology with its enormous storage volumes. It will be interesting to see if this method gives the same results as 7.3.1.

The input of the converter is fed with one "Dirac pulse". This is a pulse with infinitely large amplitude and an infinitely short pulse length but with a constant pulse area of "1" e.g. 1V x 1 second. Such a pulse exhibits a constant amplitude spectrum (constant spectral power density) containing all frequencies; it affects a circuit in the same way as a sweep generator with a constant output voltage swept through the complete frequency range.
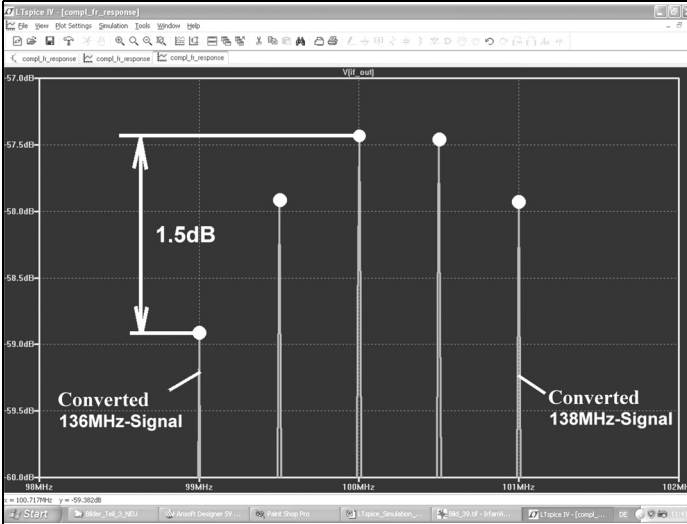
Fig 43: The transmission curve showing the passband can be seen but unfortunately the centre frequency is shifted up.

Practically the pulse will need to be longer. So the pulse length for a "practical" pulse to be used for measurements must simply be below this value:

$$t_{pulse} = \frac{0.01}{System cutoff frequency}$$

This gives an almost constant spectral power density up to the cutoff frequency of the system. The system does not notice that this is not a genuine Dirac impulse. The trick for linear systems is to make the pulse amplitude smaller so that it does not damage the circuit. The pulse response is also smaller but in principle the same curve and the frequency response can be calculated afterwards mathematically from the pulse response by convolution.

Practical test:

The converter is to be tested up to 200MHz. So the pulse length must be smaller than 1% of 1/200MHz = 1% of 5ns = 50ps. The rise and fall time of the pulse should be 1 to 2% of the pulse length e.g. 1ps each. A pulse amplitude of 10V might not harm the circuit but the pulse should be applied when everything is at idle. A simulation duration of 20µs is used (gives a frequency resolution 1/20µs = 50kHz) with a pulse start delay of 10 µs.

And with the "Maximum Time Step" of 10ps the program cannot ignore or oversee the Dirac pulse which is 50ps long. Switch the data compression off and confirm "Gear control" and you are ready to go.
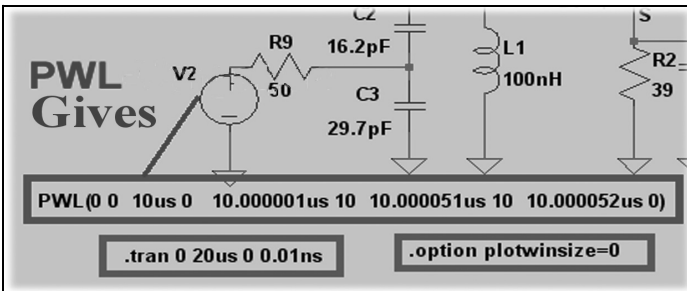

Fig 44: Programming the Dirac pulse using a PWL signal must be done carefully (Entering many zeros after the comma seems sometimes to be a problem for the user.... my own experience...).
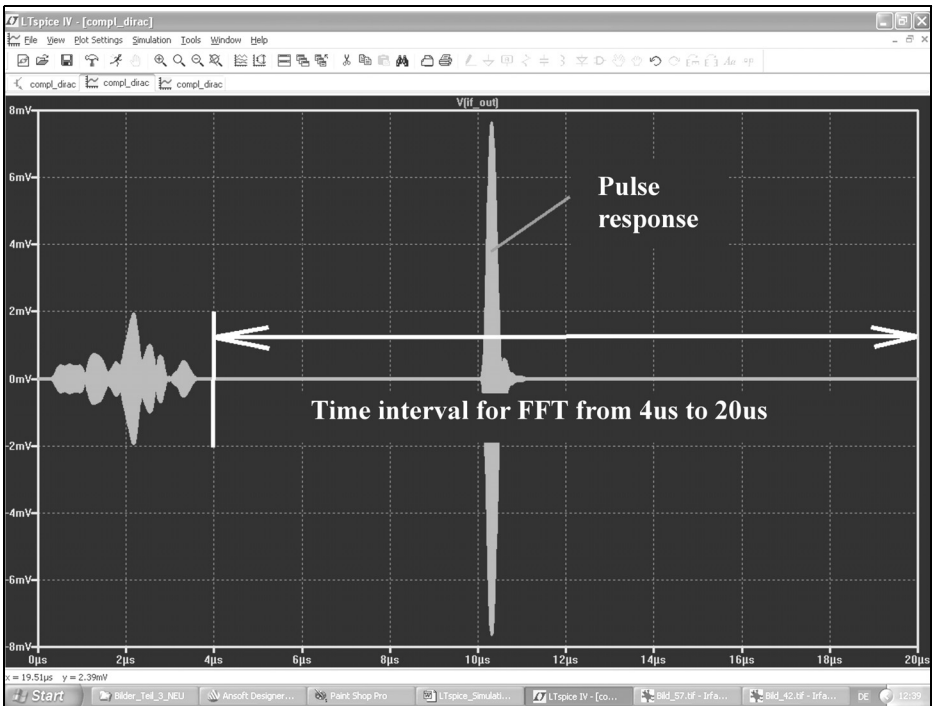
Fig 45: This is the complete output signal but an FFT time slot must be chosen to ignore the settling time before idling.

But caution:

First of all, this gives a very long computing time (approximately 20 minutes

Fig 46: It is necessary to use the Hamming windowing function for this time slot.

with a 2GHz computer) and an enormous result file of somewhat more than 1Gb because with these parameters at least 2,000,000 samples are generated and for every sample and for every node in the schematic, current and voltage must be calculated and stored.

Programming of the Dirac pulse is in the form of a PWL signal as shown in Fig 44. In addition the simulation defaults can be seen in this Fig and data compression is switched off. Finally look at the following: the key with the hammer on the control panel displays the SPICE record sheet; make sure that the "Gear" integration method is checked. In the case of this complex simulation it would be annoying if this were not pre-programmed. But now everything is ready; the simulation can be started and then just wait. A view of the output voltage in
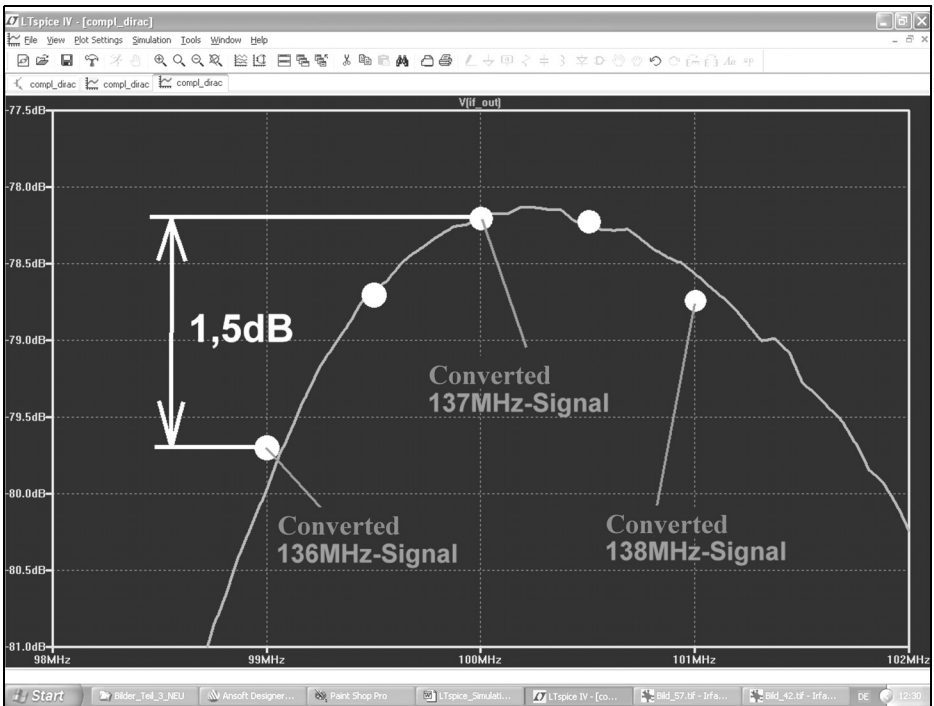
Fig 47: How about that? Such a perfect agreement between two completely different simulation methods is a joy.

Fig 45 is interesting because during the first 3µs a lot happens in the circuit: The capacitors charge themselves, currents rise, voltages oscillate around the operating point. This transient after the start is of no interested for the FFT and must be ignored for the FFT calculation. So a time slot from 4µs to 20µs is selected to get the pure pulse response. The setup menu for the FFT is shown in Fig 46, it shows:

- The time interval must be selected in the range from 4µs to 20µs
- An additional Hamming Window Function is applied to this time slot to dampen the errors caused by the abrupt changes at the beginning and end of the slot.

Finally the FFT is run with 131,072 points. The result shown in Fig 47 is interesting because the same frequency and amplitude range is shown as for the simulation in the preceding chapter (compare with Fig 43). If the measured values from the previous chapter are compared with the new diagram there are really only minimum differences between both methods. In addition, the simulated wide spectrum view of the response shown in Fig 48 is the purest joy.

So the Dirac pulse is a really fascinating thing!

7.4. Large signal behaviour and the IP3 point

Suddenly this is not simple because there are two stages in the circuit in the form of the preamplifier and the mixer that are inclined to produce more distortion with rising signals. A completely new and outstanding publication [7] dedicates a chapter to this problem and points out:
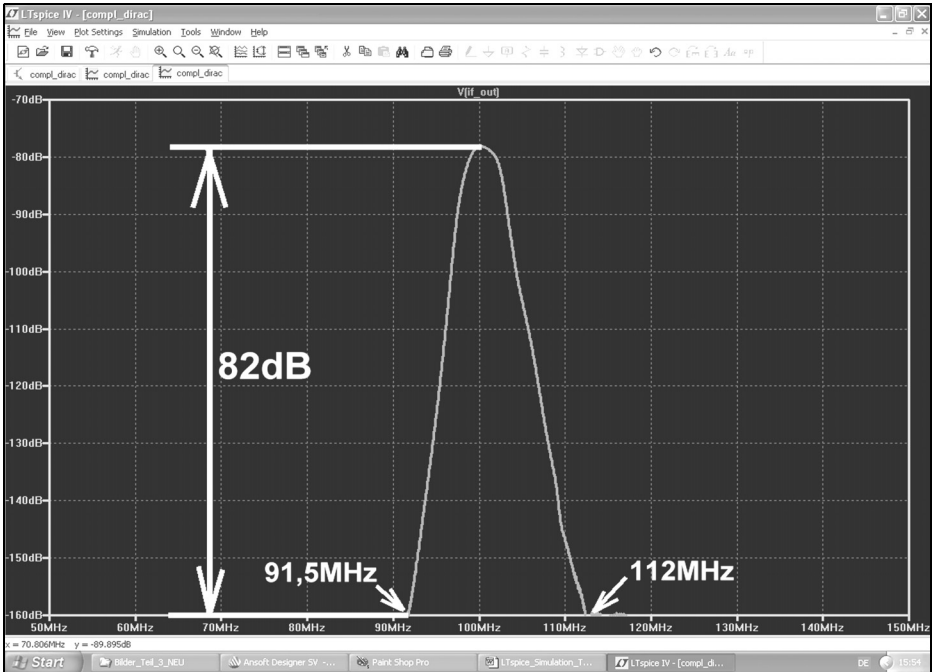
Fig 48: Another advantage of the Dirac method is that a wide spectrum view is immediately available.

- Crazy effects can occur with increasing input voltage because the individual stages exhibit different distortion behaviour and different limiting points. E.g. the IP3 product does not increase if the input signal is increased because the preamplifier or mixer run into the limiting:
- One IP3 signal suddenly decreases in amplitude and the other one rises because filter cutoff points affect the two input signal amplitudes differently.
- Dependent phase shifts occur in the individual stages. So in the sum of the intermodulation products of the different stages will reinforce or weaken one another.

Studying of this book is therefore really interesting and recommended. The whole thing quickly becomes very unclear and in the long run the only reasonable method is:

- Begin the IP3 simulation with so small input levels that the signal-to-intermodulation ratio is approximately 60dB, and then increase the input levels by steps of 10dB. After each simulation check if the input level rise of 10dB has caused an increase of the IP3 products of 20dB.
- Begin with an input level (incident wave) of -60dBm for both signals; this is an RMS value of 0.224mV or a peak value of 0.3168mV. Therefore the two signal sources for the IP3 measurement must be set to the twice peak value (0.6336mV) as unloaded voltage.

The signal frequencies are 137MHz and 137.5MHz i.e. a frequency spacing of 500kHz. The "Maximum Time Step" remains unchanged with a simulation time of 20µs with a resolution of 0.1ns giving 200,000 genuine samples. The data compression is switched off and the
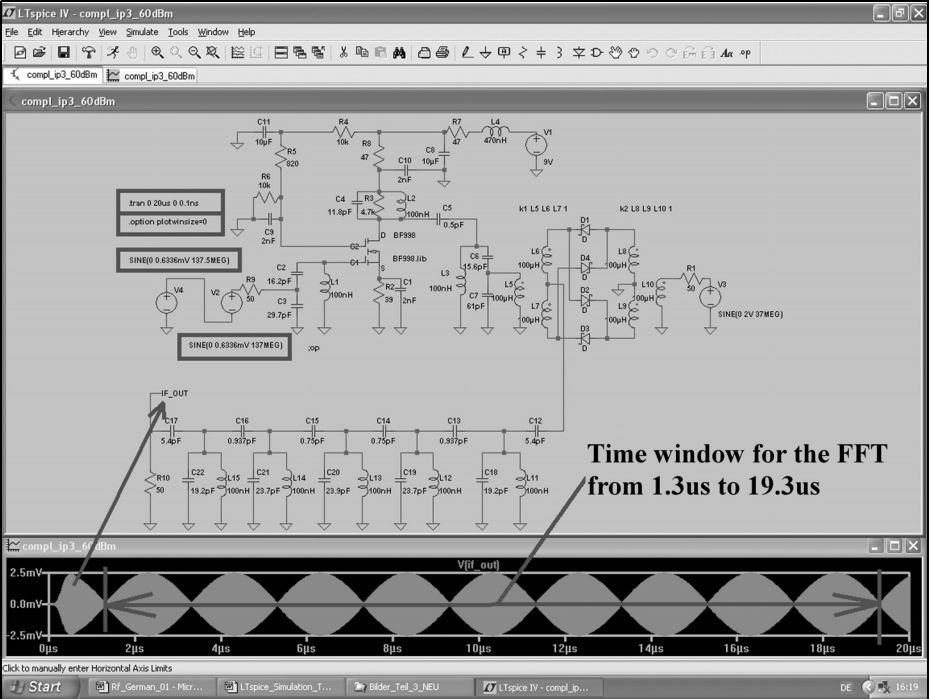
Fig 49: The complete circuit used to measure IP3 is familiar.

"Gear" parameter must be checked again.

The simulation results in the time domain are shown in Fig 49 with the complete circuit diagram. The correct time window for the FFT is set from 1.3µs to 19.3µs.
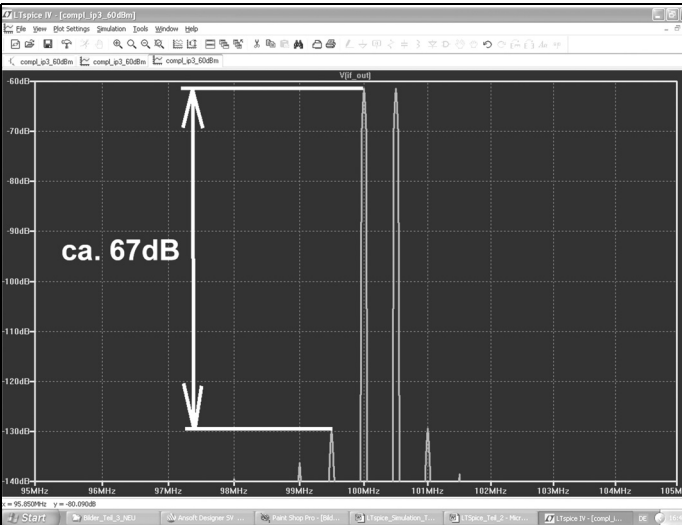

Fig 50: There are not many unwanted signals with this small input level (-60dB). It is remarkable that the simulation works correctly over such an enormous amplitude range.
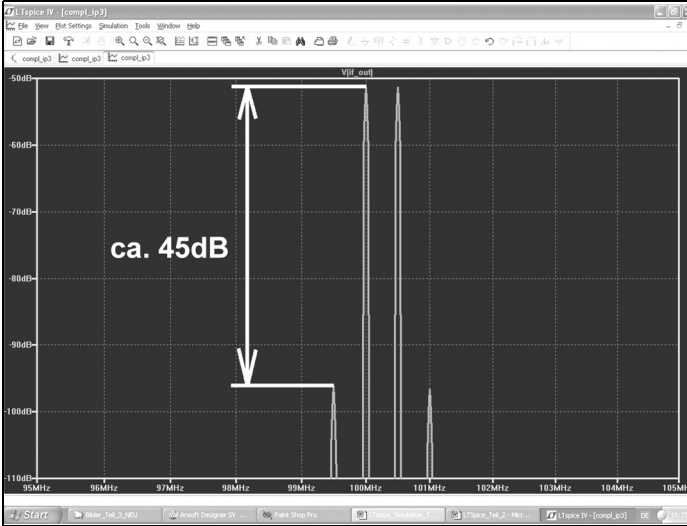
Fig 51: Nearly a text book result: 10dB increase of the input level from -60dBm up to -50dBm decreases the distance to the Intermodulation products by nearly 20dB.

This gives a result with 131,072 samples as shown in Fig 50 showing approximately 67dB between the input signal and the IP3 product.

Now repeat the simulation with a peak value of the input signals that is 10dB larger (an "antenna level" of -50dBm). This is 2mV peak input voltage and the signal-to-intermodulation ratio falls from 67dB to 45dB (Fig 51). That more or less follows the well-known law. Only if the input levels are increased again by a further 10dB to -40dBm and then by another 10dB to -30dBm are the unpredictable bad effects seen (Fig 52 and Fig 53). The limiting begins, and the intermodulation products of the preamplifier and mixer start to add or subtract in an unexpected manner.

- Sometimes the distance does not decrease suddenly, although it should. But it affects another line in the spectrum that appears unnaturally strong or attenuated.
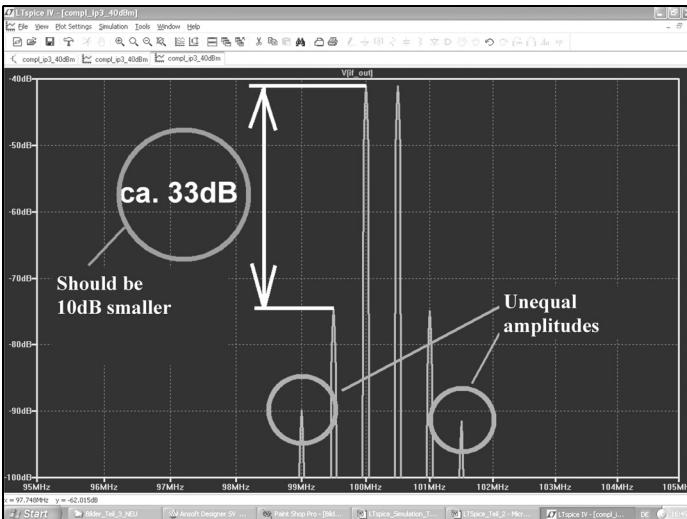
Fig 52: But with -40dBm at the input it is slowly moving away from the text book result.
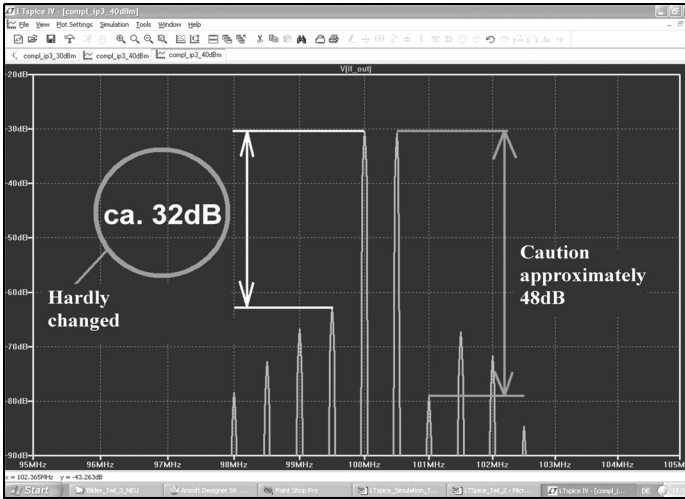
Fig 53: and for -30dBm input the circuit is completele oveloaded.

- Or the distance is suddenly worse on the left side compared to the right side.
- Or the IF output level can remain constant - etc.

Therefore the antenna voltages that can be used without bad distortion are now known quite precisely.

7.5. Noise figure of the complete converter

LTspice cannot be used for this task because of the mixer in the circuit. The program can only deal with spectral noise densities in the frequency range and due to the frequency conversion in the mixer stage the AC sweep is not applicable. Before spending a long time looking for a solution, it goes like this:

- Just use the method used by our fathers; the simple formula for "Cascaded Noise Figure" (total noise figure of the components connected together):

$$F_{total} = F_1 + \frac{F_2 - 1}{G_1} + \frac{F_3 - 1}{G_1 \cdot G_2} + ...$$

This does require some work because not only is the noise factor "F" needed but the amplification "G" is needed of each

stage - unfortunately not in dB, but as a numerical ratio.

The preamplifier:

The simulated noise figure is 0.64dB

$$F_1 = 10^{\frac{0.64}{10}} = 1.16$$

and a gain of 25dB

$$G_1 = 10^{\frac{25}{10}} = 316$$

The mixer:

As an ideal component it has an attenuation of approximately of 4.5dB

Power amplification:

$$G_2 = 10^{\frac{-4.5}{10}} = 0.355$$

Noise factor (reciprocal of the power gain

$$F_2 = \frac{1}{G_2} = \frac{1}{0.355} = 2.82$$

Continued on Page 35

Index of Volume 42 (2010)

Oscillators

A complete index for VHF Communications Magazine from 1969 to the current issue is available on the VHF Communications Magazine web site - http://www.vhfcomm.co.uk. The index can be searched on line or downloaded in pdf of Excel format so that it can be printed or searched on your own PC. If you are not connected to The Internet you can write to or fax K.M. publications for a printed copy of the index which will cost £2.50 plus postage.

Why not keep your magazines tidy with the new style Blue Binder

VHF Communications Blue Binders have been available for many years. The supplier used for many years closed down so a new supplier was found to produce the binders at beginning of 2010. These binders are the same size as the previous version but have a number of new features:

- They still store your magazines safe and tidy. Each Blue Binder holds 12 magazines.

- The magazines are held in the binder using a wire clipped into slots at the top and bottom of the binder and positioned in the centre page of the magazine. This means that individual magazines can be added or removed easily.

- The new binders have the logo and name embossed on the spine.

- The new binders have three place markers embossed on the spine to take self adhesive date labels. A strip of date labels from 2007 to 2013 is supplied with each binder.

The Blue Binders are £6.50 each plus postage. Postage is £0.90 in The UK, £1.90 for surface mail, £2.20 for air mail to Europe and £3.60 for air mail outside Europe. You can order Blue Binders using:

- The order form on the web site - www.vhfcomm.co.uk

- Fax +44 (0)1843 220080

- Post K M Publications, 503 Northdown Road, Margate, Kent, CT9 3HD, UK

VHF Communications Back Issues Available

Year	Q1	Q2	Q3	Q4
2010	Y	Y	Y	Y
2009	Y	Y	Y	Y
2008	Y	Y	Y	Y
2007	Y	Y	Y	Y
2006	Y	Y	Y	Y
2005	Y	Y	Y	Y
2004	Y	Y	Y	Y
2003	Y	Y	Y	Y
2002	Y	Y	Y	Y
2001	Y	Y	Y	Y
2000	Y	Y	Y	Y
1999	Y	Y	Y	P
1998	Y	Y	Y	Y
1997	Y	Y	P	Y
1996	Y	Y	Y	Y
1995	P	Y	Y	Y
1994	Y	Y	Y	Y
1993	Y	P	P	P
1992	Y	Y	Y	Y
1991	P	P	P	P
1990	P	P	P	P
1989	P	P	P	P
1988	P	P	P	P
1987	P	P	P	P
1986	P	Y	Y	Y
1985	Y	Y	Y	Y
1984	Y	Y	Y	Y
1983	P	P	Y	Y
1982	P	P	P	P
1981	P	L	P	P
1980	P	P	P	P
1979	P	P	P	P
1978	P	P	P	P
1977	P	P	P	P
1976	P	P	P	P
1975	P	P	P	P
1974	L	P	P	P
1973	P	P	P	P
1972	P	P	P	P
1971	P	P	P	P
1970	P	P	P	P
1969	P	P	P	P

Key: Y = Available as "real" magazines   L = Low quantity   P = Photocopy
The back issue sets contain issues marked Y. Issues marked L or P must be ordered separately.

- Single issues from 1969 to 2009, £1.00 each plus postage
- Single issues from 2010 volume, £4.70 each plus postage
- Complete 2010 volume, £18.60 plus postage
- Back issue set of "real" magazines up to 2009 (79 magazines), £60.00 plus postage
- Back issue set of "real" magazines up to 2010 (83 magazines), £75.00 plus postage
- Back issue DVDs available for the 70s, 80s and 90s magazines, £20.00 plus postage, see advert
- Back issue DVD for the 00s (2000 - 2009) magazines, £35.00 plus postage, see advert
- **Bumper DVD all magazines 1969 - 2009, £85.00 plus postage, see advert**

K M Publications, 503 Northdown Road, Margate, Kent, CT9 3HD, UK.

Tel / Fax +44 (0)1843 220080   Web site http://www.vhfcomm.co.uk

The Bandpass filter with a transmission loss of 8dB:

Power amplification:

$$G_3 = 10^{\frac{-8dB}{10dB}} = 0.158$$

Noise factor (reciprocal of the power gain)

$$F_3 = \frac{1}{G_3} = \frac{1}{0.158} = 6.3$$

Then it becomes exciting:

$$F_{total} = F_1 + \frac{F_2 - 1}{G_1} + \frac{F_3 - 1}{G_1 \cdot G_2} = 1.16 + \frac{2.82 - 1}{316} + \frac{6.3 - 1}{316 \cdot 0.355} = 1.16 + \frac{1.82}{316} + \frac{5.3}{112.18} = 1.16 + 0.0058 + 0.047 = 1.21$$

Thus the noise figure "NF" is:

$$NF = 10 \cdot \log 1.21 = 0.83dB$$

This corresponds to a degradation of the preamplifier noise by approximately 0.2dB.

Certainly this value will increase somewhat in practice with a real mixer circuit with its higher attenuation of the real transformers and data variations of the MOSFET in the preamplifier stage. But anyway: the old rule is again confirmed that the noise of the preamplifier dominates everything - and if you have enough gain present in this stage, a following passive mixer and a lossy filter don't affect this very much with their attenuations.

8.0

Conclusion

The whole topic changed from a walk to a long march. Many new experiences were encountered that compensate for all of the effort required. Sometimes things did not work and it had to be restarted from the beginning. But all doubts about the reliability of using SPICE for RF simulations have been eliminated and each new idea worked well.
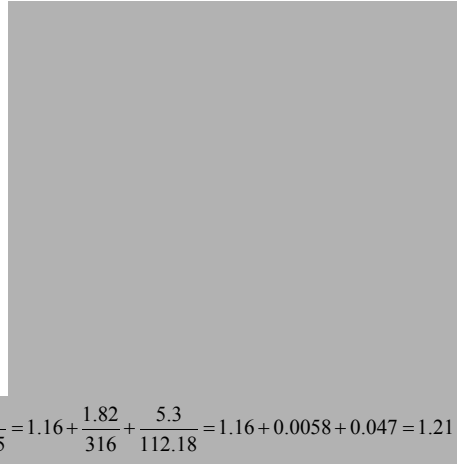
X

Literature for part 3

[5] Practical Project: Design and construction of a high quality 100MHz bandpass filter, Gunthard Kraus, DG8GB, VHF Communications Magazine 4/2003 pp 208 - 225

[6] Ansoft Designer SV project; Using microstrip interdigital capacitors, Gunthard Kraus, DG8GB, VHF Communications Magazine 2/2009 pp 78 - 95

[7]: Radio Receiver Manual, Ralf Rudersdörfer, Elektor Publishing 2010, ISBN number: 978-3-89576-224-6

Henning C. Weddig, DC5LV

The AGC module. Part 4, the search for unwanted phase errors

Continuation from 1/2010

10.0

Influence of the operational amplifiers

In order to examine the influence of the operational amplifiers and XF910 crystal filter used at the input of the AGC module on the stability of the automatic control loop, the first chain of the operational amplifiers in the AGC module with the IF amplifier was examined.

10.1 Simulation of the operational amplifier circuit

From the response time of an operational amplifier to a step function the conclusion is that the phase shift between the input and output as a function of the input frequency is far too great. The conclusion is that this phase shift contributes to the stability of the automatic control loop and helps with the choice of the values of the low pass filter R23/C17.

It is more descriptive to simulate and verify using different measurements. A Bode diagram can be used as well as the step response, this shows the gain and phase shift as a function of frequency. Programs based on the SPICE simulation are suitable for this work. Both the freeware program TINA TI [33] that is a basic version and the low priced com-

mercial version of TINA [34] have been used. The circuit to be examined is entered as a circuit diagram for both versions.

TINA TI does not have a limitation on the number of components, however at least one Texas Instruments operational amplifier must be used with the basic version; this restriction does not apply to the full version. A reduced number of components can be used with the low priced basic version. Components are building blocks for the simulation of characteristic of a circuit e.g. components with hysteresis, non linear transfer function approximated by line segments, multipliers, dividers etc as well as operational amplifiers of other manufacturers. Also a printed circuit board can be produced from the simulated circuit using TINA. It is possible to extend a simulation circuit produced with TINA TI by reading it with the basic version 7 and using the special components and simulate it without restriction.

Because no SPICE parameters were available for the CA3240 it was replaced by a TLC272.

A further possibility for the simulation is to use LTspice but this is not so simple to use.
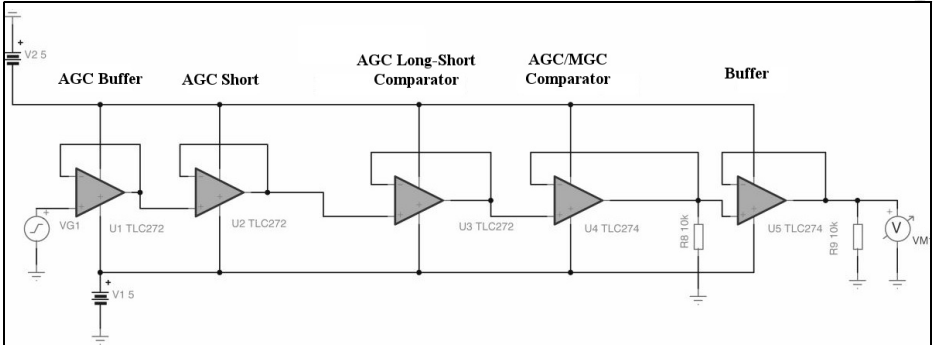
Fig 15: Simulation diagram for the AGC module using operational amplifiers.

10.2 Simulation of the AGC module

The circuit diagram for simulating the operational amplifiers in the AGC module is shown in Fig 15. Only the signal branch for AGC Short was simulated with five operational amplifiers in series. The diodes D19 and D1 were originally included in a first simulation, however the result was suspicious as it showed a non existing high-pass characteristic. The components R23/C17 were omitted for this simulation because in the first place only the transient characteristic of the operational amplifiers was to be simulated.

The input signal has an amplitude of 1V; the step response is shows Fig 16. The output signal is delayed by approximately 250ns. An overshoot of approximately 1.3V follows that corresponds to about 30% of the steady state value. The period time of the damped ringing following the overshoot is approximately 500ns resulting in a frequency of 2MHz.

The gain for all the operational amplifiers is 1 = 0dB according to Bode diagram in Fig 17. The maxima of the overshoot is +6dB (gain = 2). The period time of the ringing corresponds to the maximum gain overshoot in the Bode plot at 2MHz see Fig 17. After the overshoot the gain drops sharply, approximately 48dB measured from the peak up to a frequency of 5MHz.
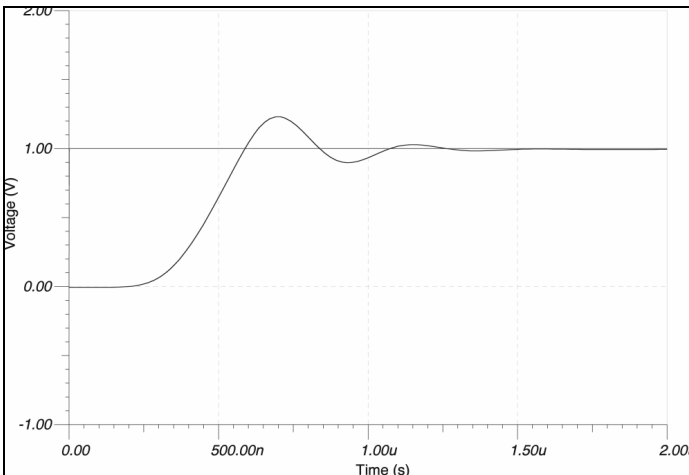
Fig 16: Simulation result of the step response for the AGC module using TLC272 and TLC274 operational amplifiers.
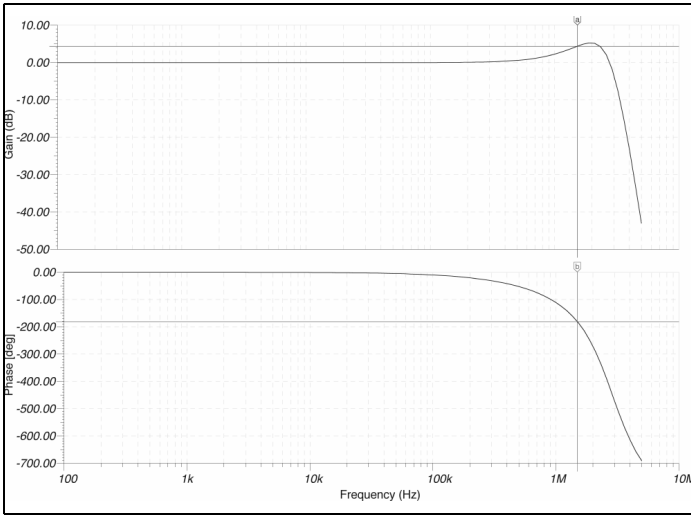
Fig 17: The Bode diagram for the AGC module with operational amplifiers. The markers show the cutoff frequency of 1.5MHz, the phase shift is -180° and the gain is +4.4dB.

The phase response is remarkably changing quickly at 1MHz and above. The cutoff frequency, when a phase shift between the input and output signal of 180° occurs, is at approximately 1.5MHz. At that point the gain is approximately +4.4dB. If the operational amplifiers were in the automatic control loop of the AGC module, the automatic control loop would be unstable!

11.0

Amplitude increased

To examine if the amplitude increase

Fig 18: Test circuit for the TLC274 operational amplifier.

shown in the simulation is possibly a simulation error a test circuit was used that can be found in: in TINA TI \Examples \TI test circuits\TLC274 "Test Circuit". A non-inverting operational amplifier is set to a gain of 2 by R2 and R3 (Fig 18). If the transient analysis is carried out on this circuit only a minimum overshoot can be seen (Fig 19). The Bode diagram (AC transfer analysis) is shown in Fig 20 and shows a smooth frequency response. The cutoff frequency (the point at which the gain falls from 6dB to 3dB) is 1.83MHz. The phase shift reaches -88° at this point. The ideal phase shift of 0° begins at <100kHz, thus smaller than 1/10 of the cutoff frequency. At twice the cutoff frequency the gain has fallen to –5.06dB and the phase shift is 130°. With these values gain falls at 9dB and a phase shift changes by 47° per octave.

If a simulation is carried out for the frequency range from 100Hz to 100MHz (Fig 21), this shows that the gain falls at 40dB per decade. The phase shift reaches -180° at 100MHz. The operational amplifier shows low-pass behaviour, this low-pass behaviour is to be examined more closely.
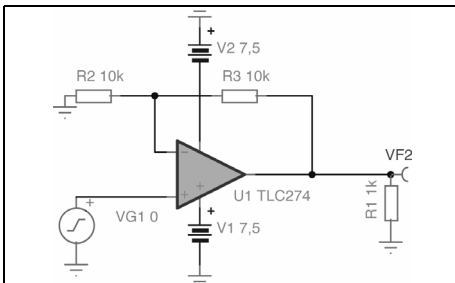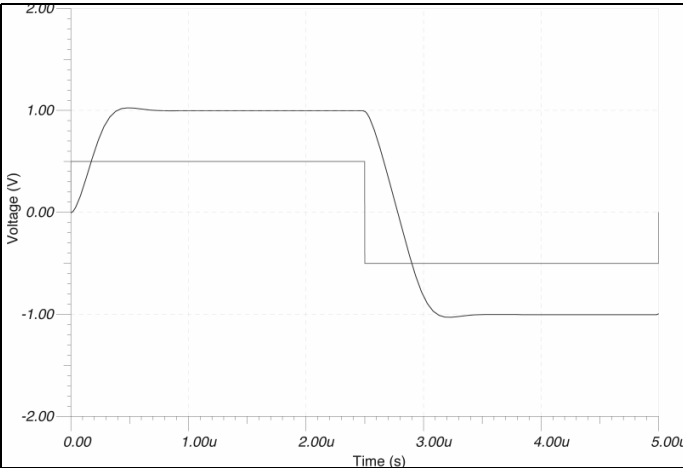
Fig 19: The step response of the TLC274 test circuit. The rise and fall time is approximately 600ns. The amplitude of the input signal is 500mV. Notice that the output signal is only half of th 0V to 1V at t=0. The over shoot is minimal.
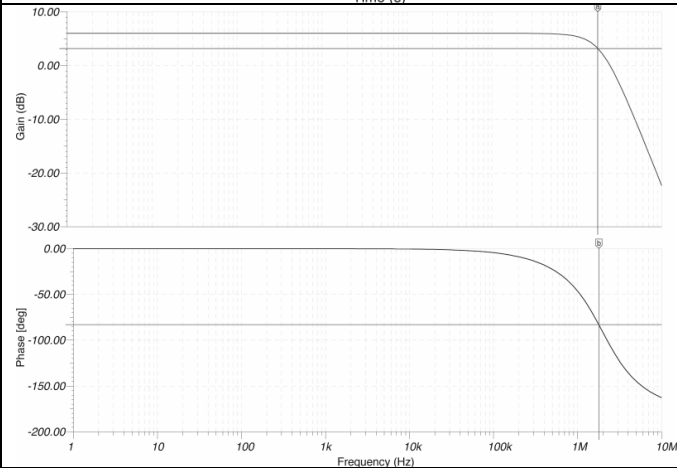

Fig 20: The Bode diagram for the TLC274 test circuit. The cutoff frequency is 1.9MHz and phase shift -80°. The ideal phase shift of 0° starts at <100kHz.
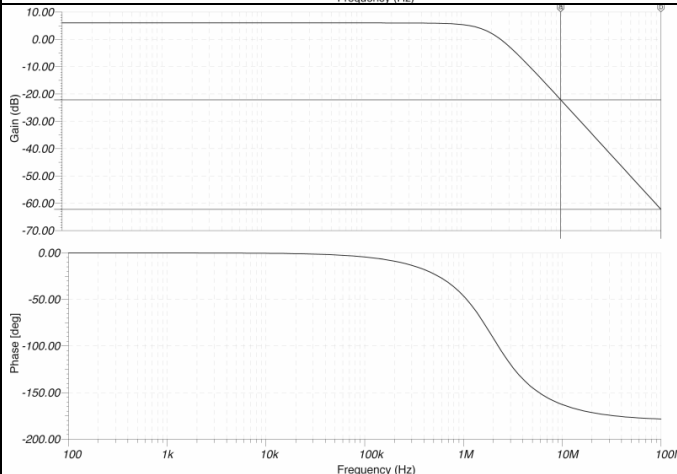

Fig 21: The Bode diagram for the TLC274 test circuit up to 100MHz. The amplitude in the area like a low-pass filter falls at 40dB per decade.The phase shift is -180° above 10MHz.
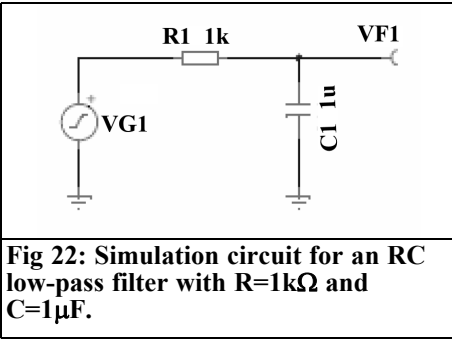
Fig 22: Simulation circuit for an RC low-pass filter with R=1kΩ and C=1μF.

11.1 Simulation of a RC low-pass filter

The original RC low-pass filter in the AGC module was R17 = 1k / C23 = 1μF, see Fig 22. The time constant of the RC element is $R \cdot C = 1k \cdot 1\mu F = 1 \cdot 10^3 \cdot 1 \cdot 10^{-6}$ V/A · As/V = $1 \cdot 10^{-3}s$ = 1ms. The amplitude of the input signal for this simulation circuit is a 1V square wave. The rise time of the RC low-pass filter, at the output, is 1ms see Fig 23. It is measured according to the definition of 0 to 63.2% (= 1 - 1/e = 1 - 1/2.718 = 1 - 0.3678 = 0.632) of the static value (here 632mV). The somewhat thicker division line on the scale represents a voltage of 625mV. After five times the time constant the steady state condition is almost reached.
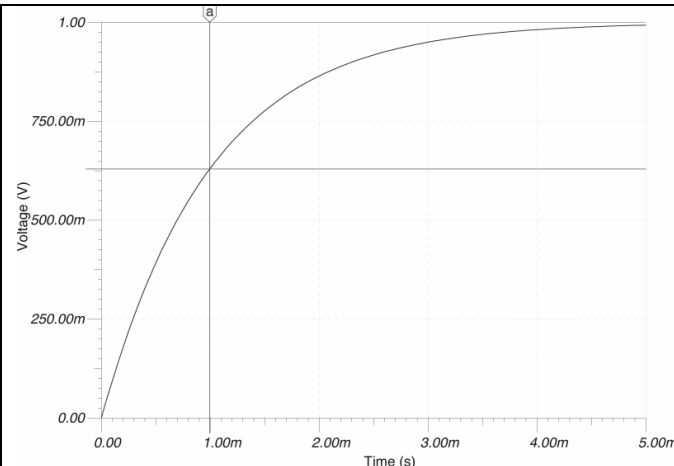
Fig 23: Step response of the RC low-pass filter with R=1kΩ and C=1μF. By definition after 1ms it has reached 63.2% of the final value. The thick line is near this at 625mV.
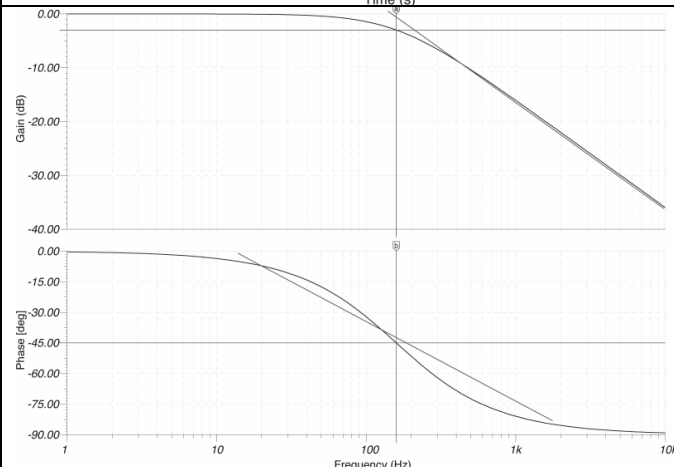
Fig 24: The Bode diagram for the low-pass filter with a cut off frequency of 159Hz where the phase shift is 45°. The attuation falls at 20dB per decade. The phase shift starts at 5.3° at 1/10 the cut off frequency and rises to 45° at the cut off frequency and is 84.3° at 10 time the cut off frequency.

The Bode diagram can be seen in Fig 24. At first sight it is amazing that the cutoff frequency (3dB point) is not 1kHz (1/Time constant), but at 159Hz. The reason is that the cutoff frequency is equal the angular frequency $\varpi = 2\pi f$, thus the value of the time constant must be divided by the factor $2\pi = 2 \times 3.14 = 6.28$. If the cutoff frequency of 159Hz is multiplied by the factor 2π it gives the frequency 1kHz. The phase shift amounts to 45°. At 15.9Hz (1/10 of the cutoff frequency) the phase shift is 5.8° and at 1.59kHz (10 times the cutoff frequency) it is 84°. The phase reaches 90° for higher frequencies. The gain slope is 20dB per decade that corresponds to 6dB per octave.

Note:
During the simulation the internal resistance of the signal source is accepted to be 0Ω, the output of the RC low-pass filter is not loaded.

11.2 The influence of a first order RC low pass filter in an automatic control loop

The phase and gain of a closed control loop are of interest for its stability. The control loop becomes unstable if the phase shift at a given frequency is 180° and the overall gain is 1. The first order low pass filter causes a phase shift of 90° at a given frequency this should be greater than ten times the cutoff frequency. Thus the low-pass filter cannot make a contribution to the possible instability by itself.

Since every system exhibits a low pass behaviour it can develop additional phase shifts that can lead to the instability if the overall gain is 1 at the appropriate frequency and the phase shift is 180°.

11.2.1 Graphic representation of the gain and phase transfer function, the so called Bode diagram

In times before the PC was available, the generation of a transfer function plot was time consuming, as for each frequency point of the diagram calculation of the gain and phase had to be done. To easy this work, a straight line approximation was invented that is explained next.

11.3 First order Low-pass filter

Approximations for the amplitude response of a first order low pass filter can be represented graphically by a straight line gradient with a slope of –20dB per decade. This straight line should be placed on a graph with a logarithmic x-axis. The y-axis should be linear scaled in dB. The x axis should be scaled logarithmically in angular frequency ($\varpi = 2\pi f$). The straight line starts at the reciprocal time constant of the low-pass filter, often called the corner frequency. The slope of this line is -20dB per decade. (for a high-pass filter the slope is +20dB per decade) The real curve for the low pass filter deviates by -3dB at the corner frequency but reaches the straight line approximation at much lower frequencies. In Fig 24 the real curve and approximation lines are included.

The phase curve is usually placed below the amplitude curve also with logarithmetically scaled frequency and linear axes. According to [35] the phase curve can be approximated by a straight line as follows:

At the cutoff frequency the phase should be -45°. At half the cutoff frequency the phase shift should be –26.6°. At double the cutoff frequency it should be –63.4°. At 1/10 cutoff frequency it should be –5.7° and at ten times the cutoff frequency it should be –84.3°.

11.3.1 Two first order low-pass filters connected in series

- Low pass-filters with different cutoff frequencies approximately a factor of 100 apart

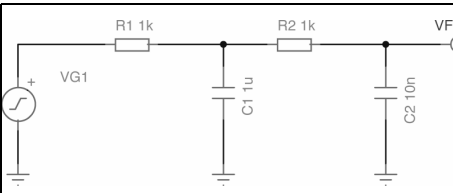 The amplitude response is a straight line with a slope of approximate –20dB per decade from

Fig 25: Simulation circuit of two RC low-pass filters in series with cut off frequencies a factor of 100 apart. R1=1kΩ, C1=1μF, R2=1kΩ and C2=10nF.

the cutoff frequency of the low-pass filter with the lowest cutoff frequency. A second straight line with the same gradient begins at the cutoff frequency of the second low-pass filter. The resulting straight line begins at the lower cutoff frequency with a gradient of –20dB per decade and bends at the higher cutoff frequency where both lines intersect to give a gradient of –40dB per decade.

The phase curves are:

The phase curve of the low-pass filter with the lower cutoff frequency is approximated by a straight line with a phase shift of -45° at the cutoff frequency, 5.7° at 1/10 cutoff frequency, 84.3° at ten times cutoff frequency and then

changing to a horizontal line at -90°. The second phase curve of the filter with the higher cutoff frequency is similar to the first phase curve. The total phase shift is the combination of both curves. A total phase shift of -180° is reached at one thousand times the cutoff frequency of the low pass-filter with the lower cutoff frequency.

- Decoupled low-pass filters with same cutoff frequency

The amplitude response comes from two curves on top of each other with a gradient of –20dB per frequency (they sum to –40dB per decade) beginning at the cutoff frequency of the low-pass filters. The attenuation at the cutoff frequency doubles to –6dB.

The phase curve is approximated by two straight lines each with a phase shift of -45° at the cutoff frequency, -5.7° at 1/10 cutoff frequency, -84.3° at ten times cutoff frequency and then changing to a horizontal line at -90°. Both phase curves overlay to give a straight line with double the gradient having a phase shift of -90° at the cutoff frequency and ignores frequencies > 10 times the cutoff
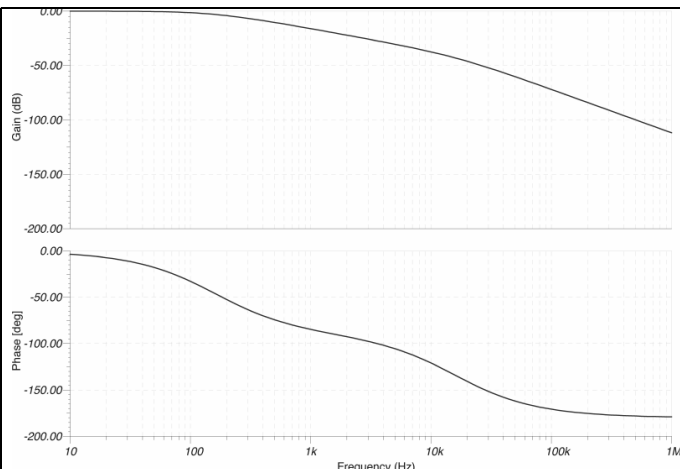
Fig 26: The Bode diagram for two RC low-pass filters in series with cutoff frequencies a factor of 100 apart. The cutoff frequencies are 159Hz and 15.9kHz. The final attenuation is at -40dB per decade.
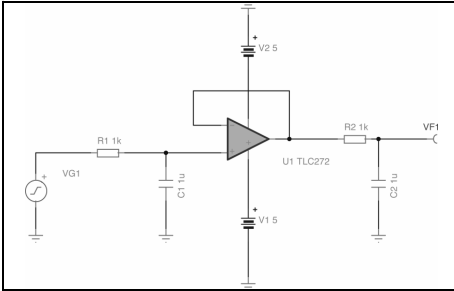
Fig 27: Simulation circuit of two RC low-pass filters with the same cutoff frequency decoupled by an operational amplifier.

frequency changing to a straight line with the phase shift of -180°.

• Non decoupled low-pass filters with same cutoff frequency

The above statements above apply at the output of unloaded RC low-pass filters. This is not true for two RC low pass filters with the same cutoff frequency connected in series. The second low-pass filter loads the first so that the attenuation is greater than –6dB.

11.4 Simulation of two first order RC low pass filters connected in series.

The appropriate simulation with TINA to support the statements about constructing graphs for the Bode diagram of multi element RC low-pass filters.

• Two low-pass filters with cutoff frequencies approximately a factor of 100 apart

The simulation diagram is shown in Fig 25. The Bode diagram of the circuit is shown in Fig 26. The straight line in the amplitude diagram has a gradient of –40dB per decade. The result of the simulation of the step response does not point to a visible difference in the rise time to the simulated step response of an individual RC low pass filter with the time constant of 1ms because the second time constant is smaller by two orders and thus only gives an error of 1%.

• Two decoupled low-pass filters with the same cutoff frequency

The simulation diagram of two RC low-pass filters with the same cutoff frequency (159Hz) connected in series, decoupled by an operational amplifier, is shown in Fig 27.

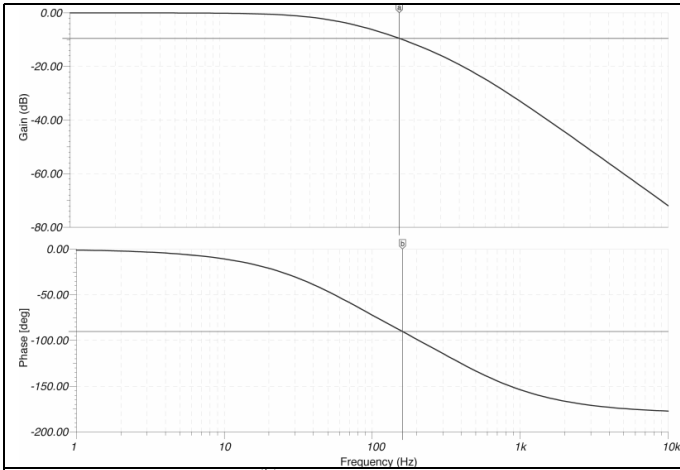The Bode diagram of the circuit is shown in Fig 28. The broken lines are the approximation to the
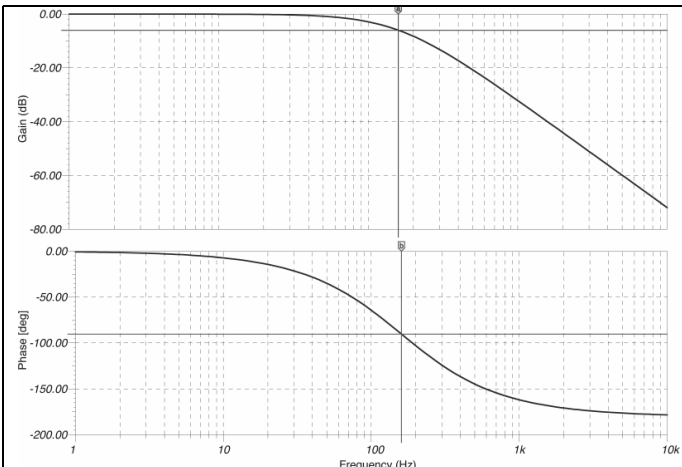
Fig 28: The Bode diagram of two decoupled low-pass filters with the same cutoff frequency.
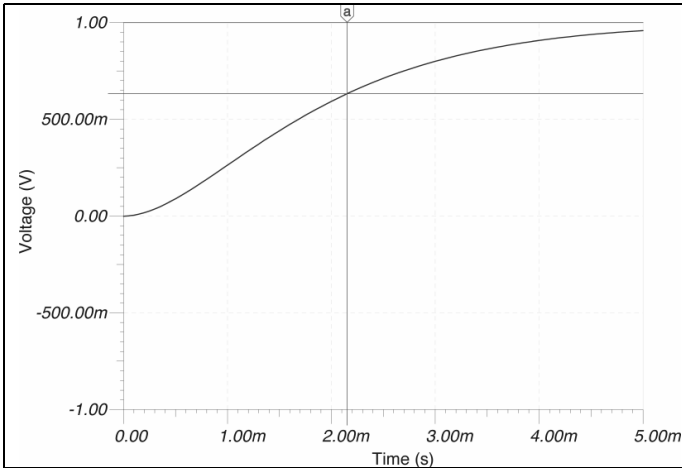
Fig 29: The step response of two deceoupled RC low-pass filters with the same cutoff frequency.

straight lines used during a graphical representation. The attenuation at the cutoff frequency is doubled at 6dB the attenuation falls off at 40dB per decade. The phase curve can be approximated by a straight line, the values doubles in relation to a single RC low pass filter: it begins with a phase shift of 2 x –5.3° = -10.6° at 1/10 of the cutoff frequency it reaches 2 x -45° = -90° at the cutoff frequency and reaches 2 x –84.3° = -186.6° at ten times the cutoff frequency. At lower and higher frequencies the value is 0° at 0Hz and -180° at > 10kHz.

The simulation of the step response, Fig 29, shows a visible difference in the rise time to the simulated step response to that of

Fig 30: The simulation circuit diagram for two RC low-pass filters with the same cutoff frequency but directly connected in series,

an individual RC low-pass filter. The step response is somewhat more than twice as large at 2.17ms.

• Two non decoupled low-pass filters with same cutoff frequency

The simulation diagram of two RC low-pass filters with the same cutoff frequency (159Hz) connected in series, these are directly coupled as shown in Fig 30.

The Bode diagram of the circuit is shown in Fig 31. The broken lines are the approximation straight lines that are used during the graphic representation.

The attenuation at the cutoff frequency increases in relation to the previous case by 3dB to 10dB attenuation is 40dB per decade. The reason for the deviation lies in the fact that the second low-pass filter loads the first. At the cutoff frequency the phase shift is 90°. The phase goes to 180° for still higher frequencies. The attenuation falls off at 40dB per decade.

The step response of both low-pass filters connected in series is shown Fig 32; the result is a time constant of 3ms but only 2ms was expected!

Fig 31: The Bode diagram of two directly connected low-pass filters with the same cutoff frequency.
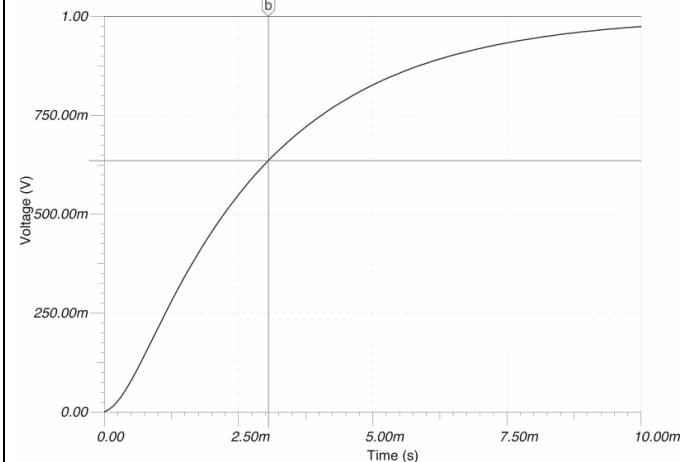

Fig 32: The step response of two directly connected RC low-pass filters with the same cutoff frequency.
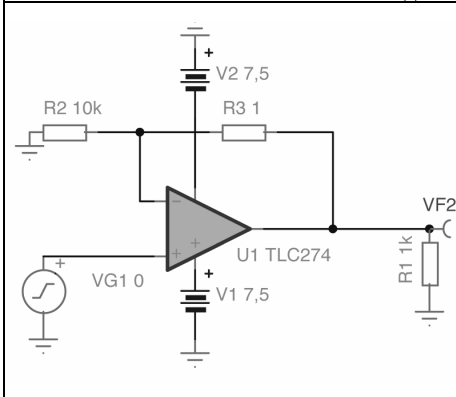

Fig 33: Test circuit for a TLC274 with a gain of 1.

The difference is caused by the load on the first low-pass filter by the second.

11.4.1 Two decoupled low-pass filters with a gain stage

As long as the amplifier exhibits a substantially higher cutoff frequency than the low-pass filters nothing changes in the phase curve within the range of the cutoff frequency. The amplitude curve is shifted up by the gain. Within the range of the cutoff frequency of the amplifier the phase shift adds. The amplitude curve amplifier changes the attenuation curve.
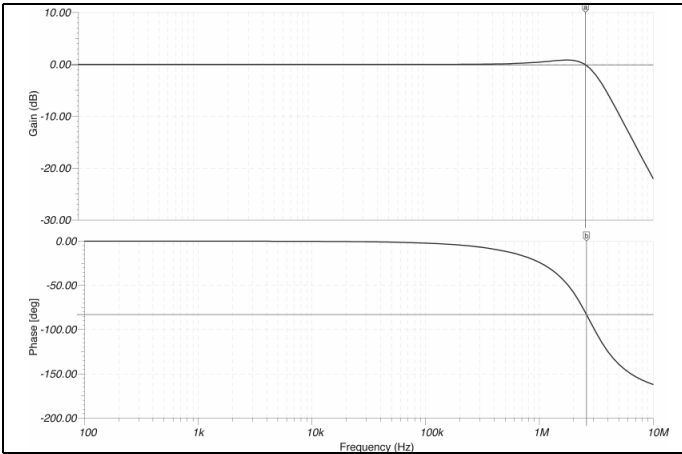
Fig 34: A Bode diagram of the test circuit for the TLC274 with a gain of 1 from 100Hz to 10MHz. The gain falls off at 40dB per decade.

11.4.2 Simulation of a TLC 274 operational amplifier with a gain of 1

The behaviour of the step response and Bode diagram changes if R3 is made smaller to 1Ω in the simulation circuit (Fig 33). Fig 34 and 35 show Bode diagrams of the simulation circuit with the upper cutoff frequency of 10MHz and 100MHz and Fig 36 shows the step response.

The maximum amplitude increase in the frequency range from 1 to 2MHz amounts to 1dB.

The cutoff frequency of the amplitude response doubles to 3.4MHz and the phase shift amounts is -110° at this frequency.

The overshoot is now much greater and amounts to 60mV, approximately 12% of the 500mV amplitude of the input signal.

The behaviour of the increased amplitude at certain frequencies and the gain of 1 can be explained by the Bode diagram. Contrary to a passive second order RC low-pass filter and the non-coupled amplifier (G = 6dB) the phase shift of the coupled operational amplifier (G = 0dB) amounts to a higher -110° thus around 20° more than a second order low-pass filter.
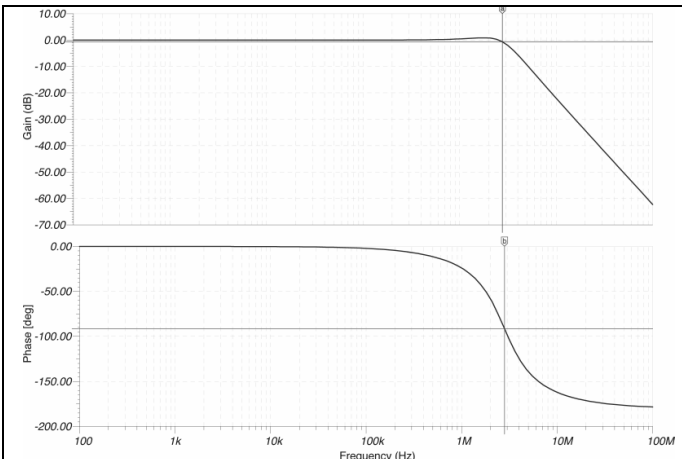
Fig 35: A Bode diagram of the test circuit for the TLC274 with a gain of 1 from 100Hz to 10MHz. The gain falls off at 40dB per decade.
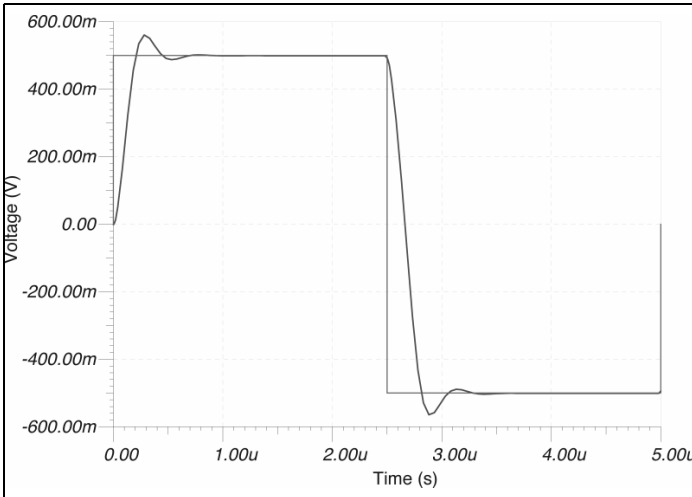
Fig 36: The step response of the TLC274 test circuit showing an overshoot of 60mV.

The operational amplifier can be compared with a control loop. The input stage of the operational amplifier is a sum-and-difference amplifier that works as a comparator stage. The signal at the output of the operational amplifier from inverted input goes through in a much shorter time than the signal from the non-inverting input of the operational amplifier. Due to this time difference, that manifests itself as a phase shift in the transfer function, an error develops by the subtraction of both signals in the comparator stage. This becomes apparent as an increased amplification.

11.5 Comparing the Bode diagram of a RC low pass filter with that of a operational amplifier

Looking at the Bode diagram of the non-coupled operational amplifier TLC 274 in the data sheet (Figure 33 [supply voltage 5V], and Figure 33 [supply voltage 10V]) it shows the behaviour of two low pass filters with very different cutoff frequencies. The open-loop gain for a DC voltage is >104 or > 80dB. Reading off the exact gain and the cutoff frequencies is very difficult due to the rough grid of the axes. The first cutoff frequency lays in the decade 100Hz to 1kHz and the second one in the decade 1MHz to

10MHz. With the higher cutoff frequency the phase shift is approximately -130°.

According to the data sheet the small signal unity gain bandwidth is 2.2MHz with a phase margin of 49° and a load resistance of 10kΩ and a load capacity of 20pF. This value depends on the supply voltage; see Figure 34 of the data sheet. The phase margin is the difference of the phase shift with a gain of 1 and the phase shift -180°. Figure 36 of the data sheet shows a diagram of the phase margin as a function of the load capacity. The phase margin drops with a load capacity of only 100pF to approximately 26°. The TLC 274 is therefore not suitable to drive larger capacitive loads.

Unfortunately the open loop gain of the TLC 274 cannot be simulated correctly with TINA or TINA TI. If the resistor R3 is omitted or increased to a very large value the gain is 30dB instead of the expected 80dB at very low frequencies! According to data sheet from Intersil for the CA 3240 this operational amplifier shows another behaviour: the open-loop gain with at 0Hz (DC voltage) is 100dB; the lower cutoff frequency is 30Hz. The open-loop gain falls starting from this cutoff frequency at 20dB per decade to a gain of one (cutoff frequency 3.4MHz). The phase shift at the cutoff frequency

(load resistance 2kΩ load capacity 0pF) is -120°, it changes to -135° for a capacitive load with 100pF and is substantially lower than the TLC 274.

The phase margin of the CA 3240 is 60° (load capacity = 0pF) and 55° (load capacity 100pF) and is more favourable with these values than the TLC 274.

12.0

Result

Originally only a short description of the simulation results and a comparison was intended. In the process of elaboration it turns out that it is meaningful to deal in greater detail with the Bode diagram. Using simple examples it can be seen, how, by means of simulation a Bode diagram can be drawn graphically without electronic aids graphically.

Measuring the transfer function of the operation amplifier chain can be carried out for ideal operational amplifiers at DC with no problem. A more exact study of the data sheet of the TLC274 could have helped to avoid this shortcoming.

The measurement setup, particularly the connection of an oscilloscope with approximately 1m long Teflon coax cable (RG188U; capacitance approximately 100pF plus approximately 30pF input capacity of the oscilloscope) in place of a 1:10 probe (approximately 12pF) on the output of the operational amplifiers in the AGC and IF amplifier modules must be analysed because operational amplifiers being measured react with additional stability problems because of the capacitive load of the measurement setup. In control theory the load capacitance together with the finite output resistance of the operational amplifier results in an extra (and unwanted) pole of the transfer function.

The capacitive load of the measuring

instrument can be uncoupled using a 100Ω resistor (R58) in series with the output of the last operational amplifier (IC5c) and the output of the AGC module (St5). It is doubtful if this value is sufficient and reliable for measurements at high frequencies (in the range 100kHz to 1MHz) because of the ability of the TLC274 to drive low impedance loads.

Naturally there are other operational amplifiers that work into the GHz range and can also drive low impedance loads, however these are usually only in SMD packages. The author found an amplifier that is capable of being driven to the negative rail, can drive relatively high capitative loads and has am moderate hiher gain bandwidth product (10MHz). These are the TLC2072 and TLC2074 operational amplifiers used in the text. The DIL package versions of these are readily available.

The author will include the operational amplifiers in the tests of the measured transfer functions of the AGC and IF module amplifier chains. It will be interesting to see how good the simulation an real measurement correlate. To be continued in part 5.

X.

Literature

[33] Simulator TINA TI; Texas Instuments

[34] Simulator TINA; www.designsoftware.com

[35] Feedback control system analysis and Synthesis; D´Azzo & Houzis; Second Edition; McGraw-Hill Book company

John Fielding, ZS5JF

Design of band pass filters

1.0
Introduction

Band pass filters are needed for various items in radio frequency engineering. These items might be receivers, transmitters and transverters. The optimum type of band pass filter is determined by several parameters, which often are conflicting. The essential parameters are:

- Centre frequency
- Bandwidth (usually measured at the –3dB points)
- Pass band ripple
- Insertion loss
- Attenuation (at some point removed from the centre frequency)
- Impedance match (input and output)
- System impedance

It should be noted that all LC (inductor and capacitor) filters use the properties of reactance to achieve a certain aim. Whether they be band pass, low pass or high pass we use the variable reactance versus frequency to fulfil our requirements. Within the pass band the impedance seen by the signal source is resistive, but out of the pass band it is highly reactive, and exhibits a high SWR. It is the reflection of the signal out of the pass band that provides the attenuation.

2.0
Selection of a topology

The selection of a topology also affects these parameters to some extent. For example, a top-coupled filter generally has a poorer attenuation response on the slope above the centre frequency than the slope below the centre frequency. On the low side the attenuation is better for offsets from the centre frequency but on the high side the attenuation increases more slowly. This is due to the filter acting like a high pass filter on the higher frequencies.

If Fig 1 is studied you will see that for equal frequency offsets from the centre frequency the attenuation per step on the lower frequency side is greater than the upper frequency side. At 10MHz offset on the lower frequency side the attenuation is 30dB but at the same offset on the higher side it is only 25dB. This top coupled band pass filter uses a trick to improve the response we will discuss later.

If the value of the top coupling capacitor is too large the response breaks up into a double humped shape; we call "*over-coupling*". This is illustrated in Fig 2, which is a 2m receiver front-end filter.

The double humped response also shows
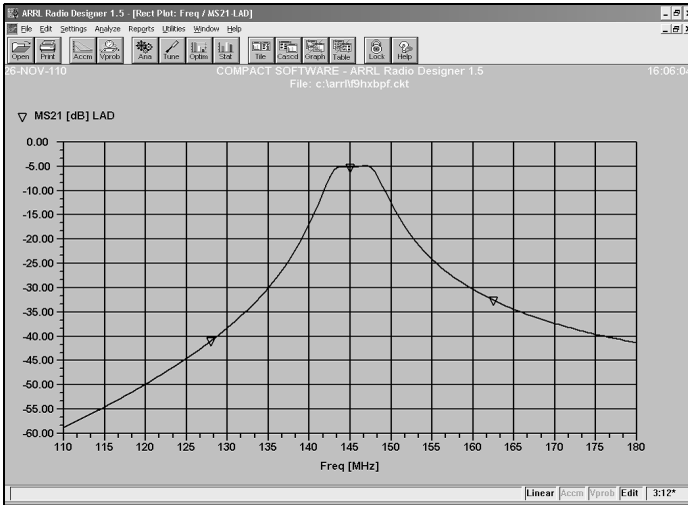
Fig 1: Typical response of a top coupled band pass filter.

a much wider bandwidth than desired and an excessive amount of ripple and insertion loss. For the demonstration filter in Fig 2 the top coupling capacitor has a value of 1.2pF. This is already a small value and the optimum coupling (Fig 3) hence requires a capacitor less than this value. Common capacitors are only available down to 0.47pF, anything less than this means we need to pull a few tricks.

For this optimised response the top coupling capacitor is now only 0.16pF, which is not commercially available. We can make such a very small value in a number of ways. One of the simplest is to wind a few turns of enamelled copper wire with a few twists and then trim the length until we get the required response, a bit hit and miss. This is known as a "*gimmick capacitor*". Alternatively we can connect several low value capacitors in series to achieve the correct value, again not very attractive, as the stray capacity could be greater than the desired value. If we connect three 0.47pF chip capacitors in series we should achieve
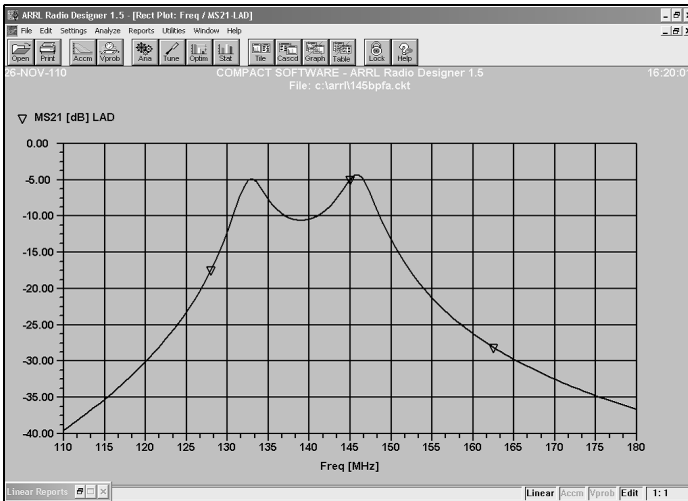
Fig 2: Over-coupled response.
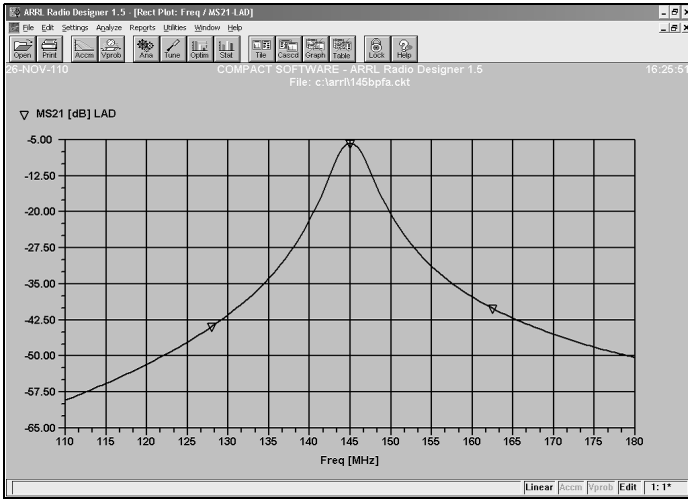
Fig 3: Optimally coupled filter response.

0.156pF, which is probably close enough.

If the value of coupling capacitor is less than the optimum the insertion loss increases and the slopes become steeper with a reduction in the pass bandwidth. Generally, it is preferable to have a slightly over-coupled response to achieve sufficient bandwidth to cover the band, while still attaining sufficient stop band attenuation.

There are a number of topologies used for top coupled band pass filters. These are illustrated in Figs 4 - 6. Note that in all the filter schematics the inductors are completely shielded from each other by screening cans, so there is no magnetic coupling.

The input and output matching is determined by the "*auto-transformer*" tapping into the two inductors. For the case of the system impedance being low, for example 50Ω, the tap on the inductor is close to ground. Unfortunately, this type of input matching is very difficult to analyse with common software packages and often the tap point needs to be found by trial and error, a slow process. C1 and C2 resonate the inductors L1 and L2 to the filter centre frequency and the coupling is performed by CC a low value capacitor. To overcome this problem we have several alternative choices. This is shown in Fig 5. In this method C1 is a high reactance capacitor (low value) that performs the transition from low to high
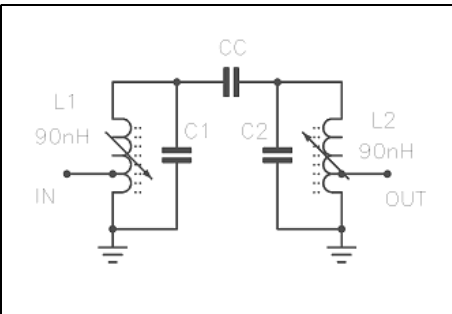
Fig 4: A tapped inductor top coupled band pass filter.
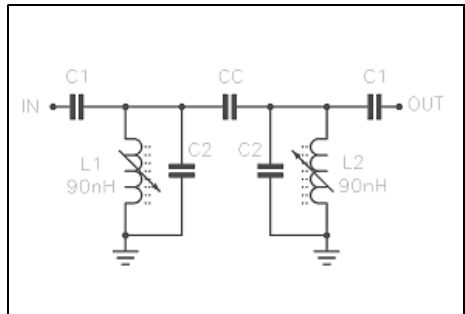
Fig 5: An alternative impedance matching method.
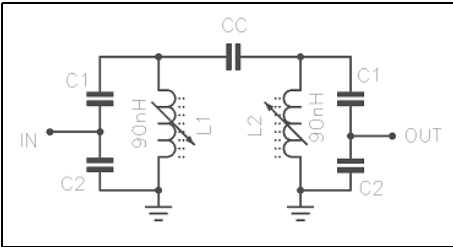
Fig 6: A method of using capacitors in series to match a low impedance into a high impedance node using a "*potential divider*" network.

Fig 7: F9HX "*bottom coupled*" band pass filter.

impedance. This now closely approximates a high pass filter and the upper slope attenuation can be expected to be worse. Another alternative is to use the concept of a potential divider to transform the low system impedance to the high impedance occurring across the parallel resonant circuit. This is shown in Fig 6. This method removes the additional high pass components in Fig. 5

C1 and C2 are two capacitors of different values. C2 is chosen so that its reactance matches the system impedance, usually 50Ω, hence it is a relatively large value. The series connection of the two capacitors also resonate the inductor to the wanted frequency, the value appearing across the inductor being less than the value of capacitor C1. If C2 is 120pF and C1 is 12pF the impedance occurring across the resonant network using L1 is roughly 11-times 50Ω, or 550Ω. This "*step-up*" in impedance also brings about a greater RF voltage across L1. The coupling between the resonant network of L1, C1 and C2 is transferred to the network using L2 by capacitor CC, and identical set of components. The filter on the output side is a "*mirror image*" of the input and the impedance occurring across L2 is transformed back down to 50Ω at the output, as C1 and C2 are the same value as the input network. The network can be visualised as being a mirror about CC, each half being the mirror image of the other.

The simple top coupled band pass filter

begins to become a headache as the frequency increases, as the value of CC gets impracticably small. There are a number of ways to solve this problem; a change in topology from top coupling to bottom coupling can also alleviate the problems. Andre Jamet, F9HX, published one method in an article in VHF Communications (3/2010) but this, although F9HX claims it is a "*bottom coupled*" method, in fact is not (Fig 7).

Although the topology offers an improvement the response still shows the classic "*high pass*" response. (This circuit was used to simulate the response in Fig 1, and although the high pass response is better than a simple top coupled filter it is still evident).

The basis of this technique is that the high reactance needed to couple between two high impedance networks in the filter is transformed down to a lower reactance in CM and then transformed back up again into the second resonant network. The basis of this design is that we are synthesising a smaller value of effective top coupling capacitor connected between the resonant networks. Although it appears to work, it in fact is not performing as well as a properly designed bottom coupled filter. For a better network we need to look at the "*Cohn Filter*" (Fig 8). This is a patented design by S B Cohn made in the 1950s. [1]

In this band pass filter the crux of the design is a combination of low pass and high pass networks cleverly aligned to give zero interference. This filter and the
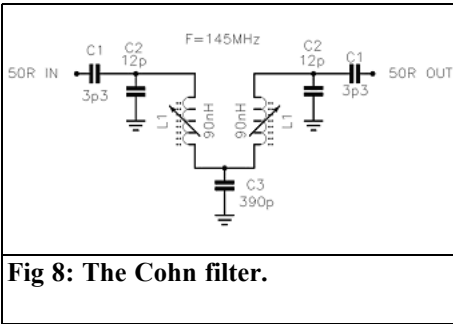
Fig 8: The Cohn filter.

other types are covered in greater detail in [2].

3.0

The Cohn Filter

The F9HX coupling is clearly not "*bottom coupled*" as claimed but a modified version of top coupling. The correct definition of "*bottom coupling*" is a link winding magnetically coupled to the bottom part of the inductors so the coupling is performed at low impedance. Another form of bottom coupling (as used in the Cohn design) is for the bottom end of the inductors to be connected together and returned to ground via a common low reactance. This is the basis of the Cohn band pass filter.

In order to fully understand the Cohn filter we need to redraw the schematic to see the design more clearly.

The Cohn filter is a mix between high pass and low pass elements. Components C1 at each end form a high pass

element; which also perform the transition from a low impedance to a high impedance, the remainder of the elements are basically low pass in nature. The component count is the same as the other topology filters, so the complexity is no greater or more costly.

The Cohn band pass filter, when the values are optimised, gives a near perfect "*mirror image*" of the response slopes either side of the centre frequency (Fig 9). A simulation of the response using a software package gives the response seen in Figure 10.

In Fig 10 can be seen the almost perfect symmetry at the low and high frequency responses. The attenuation in the stop band for various off sets from the centre frequency is identical when correctly designed and adjusted. Also the insertion loss is low at the centre frequency even when the inductors used have a less than infinite Q, in Fig 10 the mid band insertion loss is 2.5dB. The Cohn filter is the lowest insertion loss of all band pass filter designs for a fixed inductor Q. The filter in Fig 10 uses Toko 10mm variable inductors with a measured Q of only 100 at 145MHz. If a higher Q were used the pass band insertion loss becomes less, for a Q of 150 it drops to less than 2dB and the slope attenuation remains the same.

The grounding reactance can be either a capacitor or an inductor. For the inductor method it can be a few turns of wire, a SMD chip inductor or a printed coil on a substrate. The value of inductor becomes very small at high frequencies and can become a problem, but a capacitor to generate the same numeric value of reactance is quite large in value and practical.
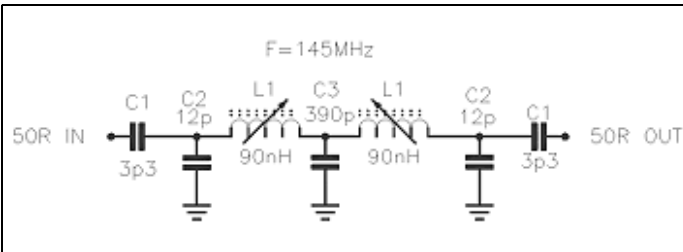
Fig 9: Redrawn Cohn filter showing the basic low pass topology.

Table 1: Some values of reflection coefficient and the equivalent SWR.

MS_{11} / MS_{22} (dB)	% reflected power	SWR
-10	10	1.93:1
-15	3.2	1.44:1
-20	1.0	1.22:1
-25	0.32	1.12:1
-30	0.1	1.065:1
-35	0.018	1.036:1
-40	0.01	1.02:1
-50	0.001	1.001

The degree of coupling is determined by the value of the common bottom capacitor, for critical coupling the value will be fairly large. As the value is reduced the filter begins to be over-coupled and the classic double-hump response is observed. For a value greater than the critical coupling the insertion loss increases and the slopes become steeper.

The other thing to be kept in mind is that any filter, be it a low pass, band pass or high pass work by generating a match to the system impedance in the pass band and a severe mismatch out of band. These filters are known as "*reflective filters*" and out of band energy experiences a very high SWR. In a high SWR the energy presented to a filter is repelled or "*reflected*" because of the large mismatch occurring. If the percentage of energy reflected is 100% then the filter presents an infinite attenuation to the signals. It is this property that allows filters to work.

If the response plot of the Cohn filter is observed in Fig 10 the trace that goes from the top towards the bottom is the input matching expressed as MS_{11}, which is the "*magnitude of the input reflection coefficient*" expressed in dB. In S parameter terms S_{11} is the input reflection coefficient, the software program adds the M for clarity to show it is a "*magnitude*" value. (The second trace is the insertion loss in dB, as MS_{21}). The larger the negative number of MS_{11} in dB, the

nearer the match is to zero reflected power, or in layman's terms closer to a SWR of 1:1.

In the plot the value of MS_{11} is -40dB, which is the same as a 20dB attenuator connected and the far end left open or short circuit. Another name for input reflection coefficient is "*return loss*", hence in an open or shorted 20dB attenuator the wave travels from the source to the other end and experiences a loss of 20dB. Upon total reflection the backward wave also experiences an attenuation of 20dB, a total of 40dB. A value of –40dB is a standing wave ratio (SWR) of 1.02:1.

The output match, known as MS_{22}, for a symmetrical filter is identical to the input match, hence MS_{11} and MS_{22} have identical values when correctly aligned. Table 1 shows some values of reflection coefficient and the equivalent SWR

For a typical filter if the reflection coefficient is –20dB or higher then the SWR can be considered acceptable.

3.1 Cascading several Cohn section into more complex filters

The basic two-section Cohn filter in some cases will not have sufficient attenuation to out of band signals. A method of improving this is to cascade two Cohn filters with an amplifier stage to provide isolation (Fig 11). A 50Ω MMIC is a simple way of doing this. The input of the MMIC is fed via a 2-section Cohn filter and the output of the MMIC feeds a second identical Cohn filter. Cascading two filters in this manner doubles the attenuation that one Cohn filter can achieve. The MMIC chosen should have a well-controlled input and output match to correctly match the filter impedance. For receiver front end filtering this is preferable to a single 4-section filter that has a higher insertion loss, as the loss before a low noise amplifier degrades the noise figure.
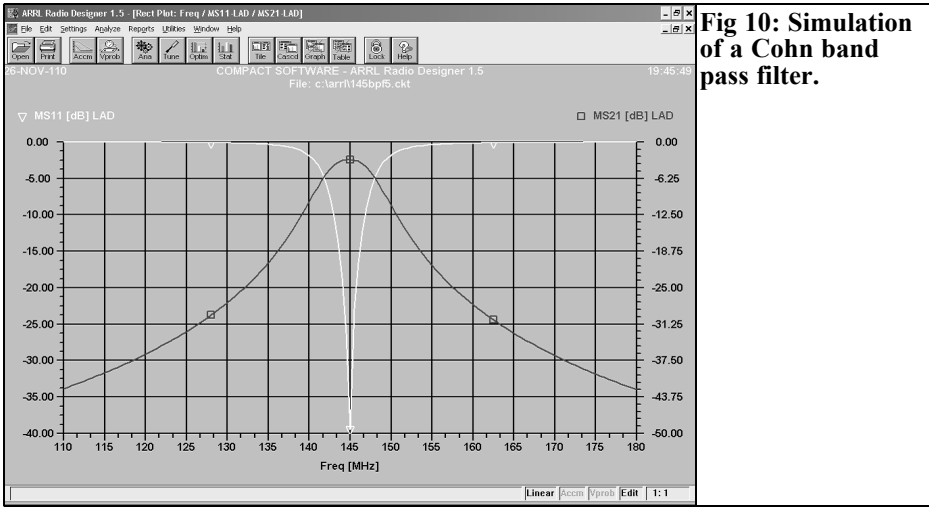
Fig 10: Simulation of a Cohn band pass filter.

4.0

Improving out of band attenuation

For top coupled band pass filters used for a receiver front end in a transceiver, there is a simple way to increase the upper slope attenuation by rearranging the block diagram. The transmitter will require a low pass filter to reduce the harmonic levels and these filters normally have very low insertion loss in the pass band. Figure 12 shows an improved method by simply moving the low pass filter to the antenna port.

The low pass filter is now connected between the antenna port and the antenna changeover relay, so it is in circuit in both the Rx and Tx paths. The high frequency cut off of the LPF combined with the Rx BPF gives much greater attenuation on the high frequency side.

5.0

References

[1] Direct Coupled Resonator Filters, S B Cohn, Proc IRE, Vol 45, pp187-196, Feb 1957

[2] RF Design Basics, J Fielding, ZS5JF, RSGB Publication, 2007
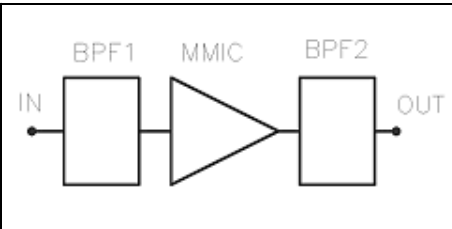
Fig 11: Cascading two Cohn filters with a MMIC buffer amplifier.
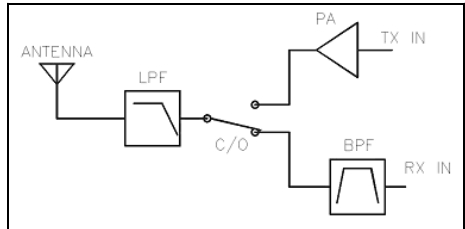
Fig 12: Rearranging the block diagram of a transceiver.

John Fielding, ZS5JF

John's Mechanical Gem 13 Tower Foundations

1.0 Introduction

Many amateurs when planning a new tower installation assume you need a massive concrete block to support the tower. Due to lack of knowledge this often entails a much greater expense, but an alternative base foundation can not only provide a stronger base but also with much less effort.

2.0 Concrete

The name "concrete" refers to a mixture of cement, sand and aggregate mixed together. The name mortar refers to just a cement and sand mix, with no other large aggregates added. Common cement is Portland cement which is mixed with various materials, the most common being sand and stone or gravel. The cement is only a type of "glue" which when cured binds the aggregates together to provide a strong foundation both in compression and tensile strength.

The concrete mixture cures by "hydration" and the ultimate cured strength is a function of the amount of moisture used to blend the various components together. The lower the amount of water used the stronger the cured concrete; hence a drier rather than a wetter mix will provide a stronger base. The compressive strength of concrete is often given in MPa (mega-Pascals, where 1 MPa = $1N/mm^2$), the higher the value the stronger the cured concrete. For an antenna tower a value of 20 to 40MPa is the optimum. For a 40MPa mix the volume of water to the other parts is optimum at 63% by volume and the cement required will typically be $300kg/m^3$ and approximately 150 litres of water/m^3. Other aggregates are small pebbles up to the size of golf balls, which are surrounded with the cement-sand mixture.

3.0 Reinforcing

For really strong foundations often a steel "reinforcing bar" structure is utilised, this is known as "rebar" and it is a high tensile steel bar, either round or square in profile, that is helically grooved to increase the contact area with the concrete. For maximum adhesion by the concrete mix the bar should have a light surface coating of rust. Hence, it is common to
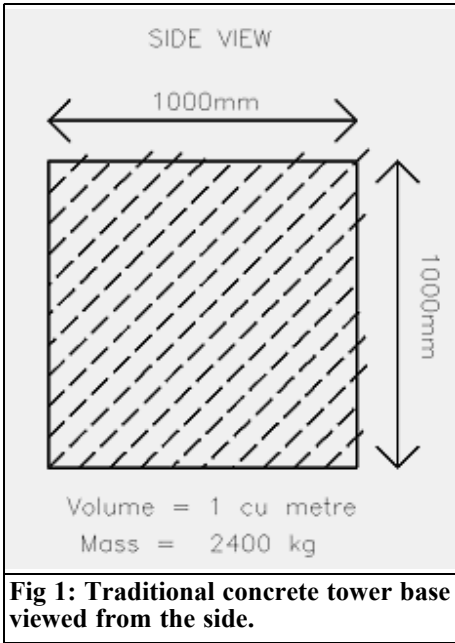
Fig 1: Traditional concrete tower base viewed from the side.
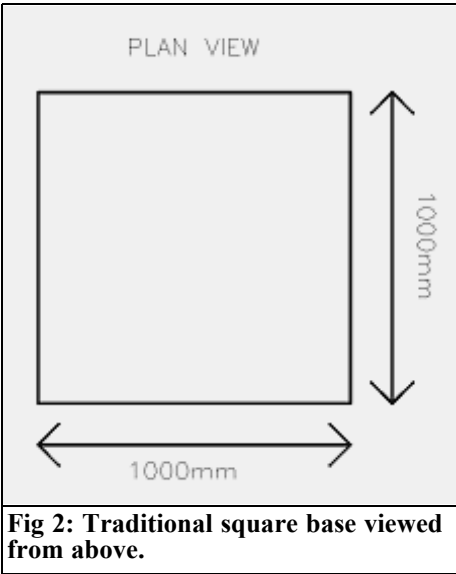
Fig 2: Traditional square base viewed from above.

find this stored in the open to promote the rusting. Pre-assembled cages made of rebar can be purchased in standard lengths for reinforcing columns or made to special order for odd shapes.

4.0

Curing time versus ultimate strength

Concrete cures by the generation of heat internally, caused by a chemical reaction within the mass to evaporate the water, leaving a solid mass. The slower the concrete dries the stronger the finished block. Hence, wetting periodically to keep the concrete damp slows down the curing and eliminates cracks due to too high a rate of curing. The wetting of the concrete can be either be sprinklers, wet sand placed on top, plastic sheeting to retain the moisture or sacking watered every day to keep the concrete moist.

The typical setting time versus ultimate strength for a nominal 40Mpa mix is shown below.

Initial setting time =   2 – 3 hours
                        (touch dry)

Final setting time =   3.5 – 4.5 hours
                       (firm to the
                       touch)

Compressive strength

3 days =   24 – 28MPa
7 days =   37 – 41MPa
28 days =   56 – 60MPa

From this it can be seen that the tower should not be erected before about 7 to 10 days have elapsed from initial pouring.

5.0

Common mix for 40MPa concrete

The recommended mix for 40MPa concrete is given by volume:
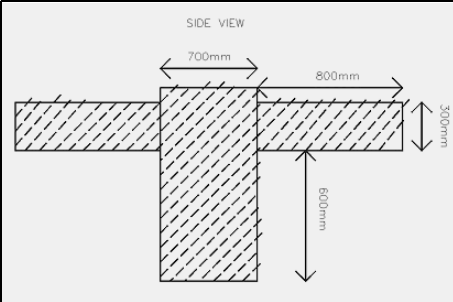
Fig 3: Improved concrete base using raft foundation – side view.

Fig 4: Raft foundation viewed from above.

Portland cement	=	1 part
Stone / Pebbles	=	3 parts
Sand	=	2 parts

The sand is referred to as "Sharp Sand" and it should be dry, clean and devoid of any salt or other contaminants which can adversely affect the final cured strength. Converting these ratios into weights of the materials we find we need approximately the following per cubic metre of concrete:

Portland Cement	=	320kg
Sharp Sand	=	600kg
Stone Aggregate	=	1200kg
Water	=	176 litres

If the sand or stone is wet then the amount of water to be added is proportionally less.

Often an additive liquid is used to promote better flow around the reinforcing bars; ordinary dish washing liquid is a good substitute at the ratio of 10ml per litre of water, as the mix should be fairly dry for maximum strength. As an indication of how the wetter mix affects the ultimate strength:

Optimum water in mix = 100% of ultimate

+10 litre per 1m³	=	80%
+20 litre per 1m³	=	60%
+30 litre per 1m³	=	40%

When mixing concrete it is better to use a bucket to measure out the required volume of the various constituents. As we can see from the above tables, the bulk of the mass is the stone, being about 50% of the finished bulk when cured, the cement is only 15% by mass.

6.0

Cured mass of 40MPa concrete

The mass of concrete varies between 2200kg/m³ up to 2500kg/m³ depending upon the aggregate type used. Hence, a typical antenna tower base using 2m³ will be about 5-tonnes in weight (Figs 1 and 2). However, it is not the dead weight that prevents an antenna tower from toppling over but how much "purchase" it has with the soil the base is cast in. We can make a considerable saving in concrete by redesigning the block shape. Most amateurs assume a hole of equal sides and depth is the best method, say 1m x 1m x 1m, which entails 2300kg of concrete when cured.

7.0

Prevailing wind

The wind typically flows from one of two opposing directions, possibly SE and NW, so the tower can be subjected to one of two opposing forces. In order to better counter these two forces we can use a

"raft foundation" which gives a considerable saving in concrete and is stronger than a simple cubic block of concrete as it has more purchase with the surrounding soil (Figs 3 and 4).

The two side arms are positioned below ground level and extend out for 800mm either side of the main block. The vertical block and the two arms are reinforced with rebar, the rebar used for the arms being continuous pieces full length running across the top of the vertical block and tied into the vertical rebars. The prevailing wind from one direction tries to overturn the tower, but the forces are resisted by one raft arm being forced into the ground and the other side is being pulled out of the ground. The volume of concrete required for the standard base shown is $1m^3$. For the raft foundation design the central block requires $(0.7 \times 0.7 \times 1) = 0.49m^3$. The two side arms require $(0.3 \times 0.3 \times 1.6) = 0.162m^3$ making a total of $0.652m^3$, a saving of 35% in concrete.

For soils with a lower strength (sandy soils) the vertical column will need to be deeper but the arms can be the same as for good soil types.

8.0

Additional reinforcing methods

As it is the "grip" the tower base exerts on the surrounding soil that prevents overturning moments, anything we can do to increase this is beneficial. One simple method is to drive into the side walls of the hole, as well as the bottom, many lengths of rebar or similar metal at varying heights from bottom to close to the top of the hole. The writer used 500mm off cuts of 25mm angle iron hammered into the soil up to half the length. These many pieces of bar sticking out into the hole when the concrete is poured more than doubles the effective

area of purchase with the soil.

If the soil depth is low and the underlying strata is rock, then "epoxy rock-bolts" should be considered for placing in the bottom of the hole. These are lengths of high tensile steel studding which are inserted into pre-drilled holes and fastened in place with two-part epoxy glue. The glue is supplied in a tubular canister that is first inserted into the hole so it rests on the bottom and then the rock-bolt is hammered down into the hole, which bursts the canister. Turning the bolt mixes the two parts until the epoxy glue is seen to rise to the top of the hole. This method is widely used in the mining industry to reinforce tunnels etc.

9.0

Tower holding down bolts

There are several different possibilities for tower holding down bolts. We can make a "cage" welded up from angle iron immersed in the concrete with bolts protruding to align with the tower bottom plate. Alternatively we can make "hook bolts" in the shape of a J with the top portion threaded to accept nuts to bolt the tower onto the tower base. (If using hook bolts then these should be made to a depth of 80% of the concrete block). Whichever method is used it is important that when the concrete is poured the alignment is maintained, it is near impossible to correct once the concrete is cured. Often a dummy template can be taken of the bottom tower section (made from plywood or similar sheet wood, with a large hole in the centre to pour the concrete through into the hole). This can be used to hang the hook bolts (with nuts to set the correct protrusion above the block), into the hole to ensure alignment whilst the concrete cures. Once cured the template can be removed and the bottom tower section then fastened in place. Failure to ensure correct alignment can
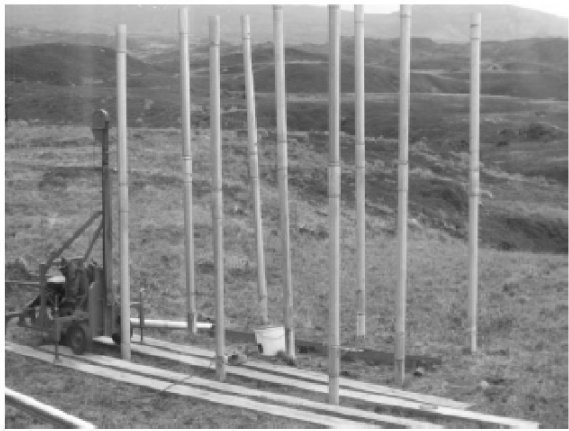
Fig 5: Erection of 15m antenna tower on Marion Island. Pictures courtesy of Pierre Tromp, ZS8M / ZS1HF.

be a serious headache to correct the error.

It is recommended that a minimum of 8.8 grade steel is used to make the hook bolts (see previous Mechanical Gems for details) as it is necessary to torque the nuts to a high value to ensure enough tensile stress in the holding down bolts. Although the bolts are in tension this is also transferred to compressive loads into the concrete block by the tower base.

10.0

Alternative to a concrete block foundation

The pictures shown in Fig 5 are an alternative method of securing a tower to the ground. These show the newly erected 15m high tower on Marion Island in the South Atlantic Ocean. The 9 vertical stainless steel tubes that form the bottom of the tower are driven into the ground with a pile driver to a depth of 2m at which depth the rock layer is situated.

Errata for John's Mechanical Gem No 12

Greg ZL3IX wrote to John pointing out an error in the wind loading value.

The force applied is a function of the square of the wind velocity. Therefore for a 80km/h wind the force on a 1m² surface is 44kgf, but for a wind velocity of 160km/h it is 176kgf and not 88kgf as stated.

Anyway it just highlights the advantage of a mesh rather than a solid surface for a large antenna.

Gunthard Kraus, DG8GB

Internet Treasure Trove

NEC2c

NEC2 is well known as simulation software for wire antennas. However it was written in FORTRAN and that is no longer in generally use. Therefore it has been "ported" too the "C" programming language (happily used by many programmers). This has also made further complex program enhancements available such as coloured graphics for results.

Address: http://5b4az.chronos.org.uk/pages/nec2.html

W1GHZ online Microwave Antenna Book

This is really a fine book: a comprehensive representation of this topic that is well written and easily understandably with the latest developments. It is a very good book for its time, the complete work of 12 chapters can be downloaded and it works

Address: http://www.w1ghz.org/antbook/contents.htm

Inside a typical SPICE file

For those who use SPICE for simulations and are interested in developing model files. For the curious it shows the suitable changes needed to adapt an existing Spice model to suit an older component.

Address: http://www.ecircuitcenter.com/basics.htm

W1GHZ 10GHz site

There are many things to discover. Among other things it is possible to download interesting practical projects and articles from QEX magazine as well as all DUBUS magazine for the period 1982 to 1992.

Address: http://www.w1ghz.org/10g/10g_home.htm

The WB0DGF Antenna Site

Again something about antennas. On this site all articles on this topic are listed. They are all worthwhile to read just look at the list for something of interest.

Address: http://wb0dgf.com/

Return loss bridge

Those who have thought of building such a measuring bridge should visit this site. There are many fundamentals explained and also practical information.

Addresses: http://www.qsl.net/n9zia/rlb/index.html

http://www.k8iqy.com/testequipment/returnlossbridge/returnlossbridge.htm

http://www.vk2zay.net/article/179

R.F.Elettronica

This is very good: You will find a company that not only supplies the latest products but also worries about the emergency requirement of developers and radio amateurs.

There is a full online catalogue of all products. This includes a genuine electronics flea market in plain language and clear pictures, with "Surplus Offers" of microwave components or complete microwave modules. There is also PCB material and all at reasonable prices plus delivery anywhere. You must visit this site.

Address: http://www.rfmicrowave.it/home.php?lang=eng

EAGLE

For those who carry out antenna measurements and are not only interested in radiation patterns. There is also impedance performance of the antenna and some beautiful Application Notes.

Address: http://www.eagle-1st.com/eagle1st.nsf/e4fa682eb52a27e10725763c007961ea/efb5f60e1d940e6507257663005b1315!OpenDocument

SHF Communication Technologies

That is a company that fights at the forefront of communications: very high frequencies and very high data rates. The Application Notes are also interesting

that describe the state of the art. These useful for further training.

Address: http://www.shf.de/en/communication/downloads/application_notes/

M/A-COM

A well-known name as a supplier of high-quality RF and microwave components. The expansion of this site is particularly interesting; the "Technical Resources" have more pages for the reader. The Technical Literature and Application Notes have block diagrams and up to the minute technical articles. A fine site and very interesting.

Address: http://www.macomtech.com/Content/technicalresources

Note: Owing to the fact that Internet content changes very fast, it is not always possible to list the most recent developments. We therefore apologise for any inconvenience if Internet addresses are no longer accessible or have recently been altered by the operators in question.

We wish to point out that neither the compiler nor the publisher has any liability for the correctness of any details listed or for the contents of the sites referred to!

VHF COMMUNICATIONS

A Publication for the Radio Amateur Worldwide

Especially Covering VHF, UHF and Microwaves

Volume No.43   Spring   Edition 2011-Q1

Back Issues on DVD

VHF Communications Magazine has been published since 1969. Up to 2002 it was produced by traditional printing methods. All these back issue have been scanned and converted to pdf files containing images of the A4 sheets that formed the A5 magazine when folded in half. These have been put together on DVD in decade sets.

From 2002 the magazine has been produced electronically therefore pdf files are available of the text and images. These have been used to produce the 2000s decade DVD.

1970s - 1980s - 1990s

These three DVDs cover the first 3 decades of the magazine. The 1970s DVD contains all magazines from 1969 to 1979 (44 magazines) the 1980s and 1990s DVDs contain 40 magazines for the decade. The DVDs are £20.00 each

2000s

This DVD contains magazines from 1/2000 to 4/2001 in scanned image format and from 1/2002 to 4/2009 in text and image format. This DVD is £35.00
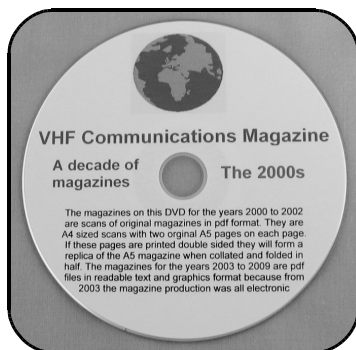
Bumper 4 decade DVD

This DVD contains all magazines from 1969 to 2009. That is 164 magazines. It also contains the full index for those 41 years in pdf and Excel format so that you can search for that illusive article easily. This DVD is just £85.00 - just 52 pence per magazine.

To order, use one of the following:

- Use the order form on the web site - www.vhfcom.co.uk
- Send an order by fax or post stating the DVD required (1970s, 1980s, 1990s, 2000s, Bumper)
- Send the correct amount via PayPal - vhfcomms@aol.com - stating the DVD required (1970s, 1980s, 1990s, 2000s, Bumper) and your postal address

    Add £1.00 for air mail postage in Europe or £1.50 for air mail postage outside Europe